Jb. Geol. B.-A.	ISSN 0016–7800	Band 129	Heft 1	S. 69–91	Wien, April 1986

Polymetamorphism of the Oetztal-Stubai Basement Complex Based on Amphibolite Petrology

By ABERRA MOGESSIE & FRIDOLIN PURTSCHELLER*)

With 12 figures and 8 tables

Tyrol
Oetztal-Stubai Complex
Amphibolites
Hornblende-Zonation
Polymetamorphism
Hercynian metamorphism
Alpine metamorphism

Österreichische Karte 1 : 50.000
Blätter 144, 145, 146, 147, 148, 171, 172, 173, 174, 175

Content

Zusammenfassung

Texturelle und mineralchemische Beziehungen lassen auf die polymetamorphe Geschichte der Ötztaler-Stubaier Amphibolite schließen. Mit steigendem Metamorphosegrad nehmen die Gehalte an Na^{A}, K, Na^{M4}, Al^{IV}, Al^{VI} und Ti ebenso wie die An-Gehalte der Plagioclase zu. Die zonierten Ca-Amphibole zeigen in Ihrer Zusammensetzung verschiedene Kern-Rand-Beziehungen zwischen Aktinolith und Hornblende, die als Hinweis für mehrere Wachstumsphasen der Amphibole gedeutet werden.

Folgendes Schema der polymetamorphen Entwicklungen kann aus den Ötztaler-Stubaier Amphiboliten abgeleitet werden:

1) Eine vor-hercynische (kaledonische?) hoch-P und hoch-T Metamorphose;
2) eine wahrscheinlich früh-hercynische Metamorphose in unterer Grünschieferfazies (Phase I);
3) eine hercynische Amphibolit-Fazies mit mittleren P- und hohen T-Bedingungen (Phase II);
4) eine altalpidische Metamorphose mit absteigendem Metamorphosegrad vom SE des Ötztales (Amphibolit-Fazies) nach NW (untere Grünschiefer Fazies).
5) Retrograde Mineralparagenesen, bedingt durch die Abkühlung nach dem Altalpidischen Höhepunkt im nördlich an den Schneeberger Zug angrenzenden Altkristallin.

*) Authors' address: Dr. ABERRA MOGESSIE, Univ.-Prof. Dr. FRIDOLIN PURTSCHELLER, Institut für Mineralogie und Petrographie, Universität Innsbruck, Innrain 52, A-6020 Innsbruck.

Summary

Based on the rock and mineral analyses and the observed textural relationships, evidence for the polymetamorphic nature of the Oetztal-Stubai amphibolites have been established. With increasing grade of metamorphism Na^{A}, K, Na^{M4}, Al^{VI}, Al^{IV} and Ti contents of the amphiboles increase. The anorthite content of the plagioclase also increases. The zoned calcic amphiboles represent various combinations of core-rim composi-

tion, i. e. actinolite-hornblende, hornblede-actinolite. These types of textural relationships are considered to indicate multiple periods of mineral growth. Thus, the polymetamorphic situation in the Oetztal-Stubai amphibolites records

1) a high P&T metamorphism of pre-Hercynian (Caledonian?) age;
2) a low grade greenschist facies metamorphism of possible early Hercynian age (phase I);
3) a low to medium P and high T metamorphism (amphibolite facies) of Hercynian age (phase II);
4) a medium P Alpine overprint whose metamorphic grade decreases from SE (amphibolite facies) towards NW Oetztal (low greenschist facies);
5) early Alpine cooling (represented by retrograd mineral assemblages in amphibolites of the old crystalline Basement bordering the Schneeberg complex to the north).

1. Introduction

Although a considerable amount of data is available on the geology, petrography and mineral chemistry of the pelitic schists or metasedimentary rock units in the Oetztal-Stubai Alps (see PURTSCHELLER, 1978 and references therein; HOINKES et al., 1982), except the geologic and petrographic studies of the amphibolites of the central Oetztal (HEZNER, 1903; HOFFER, 1967; HOERNES & HOFFER, 1973; MILLER, 1970) a complete petrographic and mineral chemistry as well as geochemical study of the amphibolites occurring in the Oetztal-Stubai Alps has been lacking to date.

The purpose of this study is to provide new data on the petrography and mineral chemistry of the amphibolites of the Oetztal-Stubai old crystalline Basement; and based on these data to try to understand the nature of the polymetamorphism in this part of the Eastern Alps.

1.1. Geologic Setting and metamorphism

The Oetztal-Stubai complex (Eastern Alps) is an overthrusted mass mainly consisting of pre-Hercynian rock series covered by mesozoic metasedimentary units (Brennermesozoikum) (see Fig. 1).

The principal para rock types are quartzo-feldspathic-biotite plagioclase gneisses, schists, calc-silicate rocks and quartzites. Rocks of magmatic origin include granitic to granodioritic gneisses, banded amphibolites, peridotites, eclogites, eclogite-amphibolites and garnet

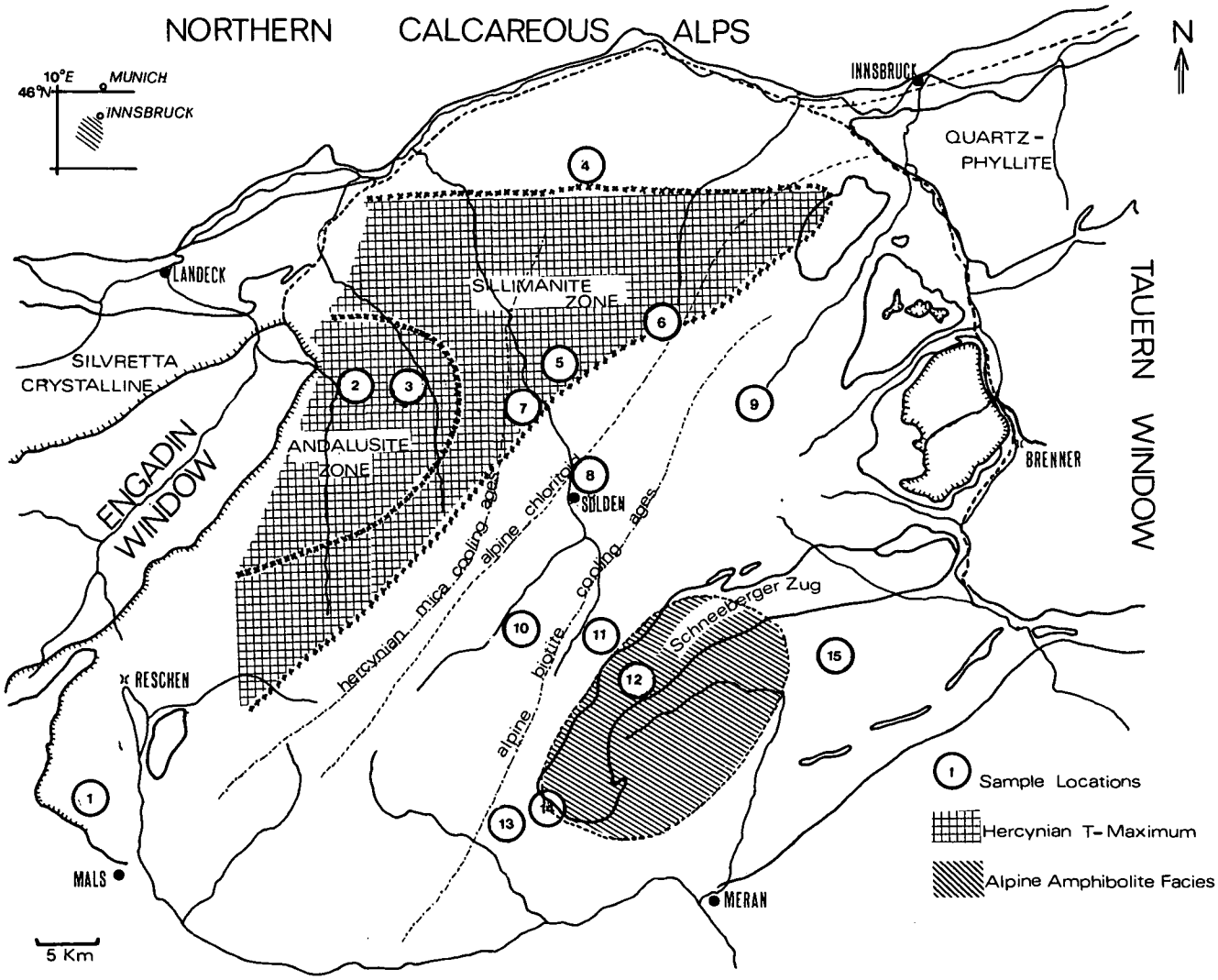

Fig. 1: Symplified Geological Sketch Map of the Oetztal-Stubai Basement, showing Hercynian and Alpine heat domes and increasing Alpine metamorphism from NW to SE, established by Hercynian mica cooling ages (THÖNI, 1980) and Alpine chloritoid line (PURTSCHELLER, 1967). Sample locations 1–4 represent those from the N/NW (Prämayur, Pitztal, Kaunertal, Kühtai, Zirmalm); 5–6 are from central Oetztal (Milchenkar, Lüsens, Pollestal, Solden); 9–15 are from S/SE Oetztal (Ranalt, Ventertal, Gaisbergtal, Rotmoostal, Schneeberger Zug, Pfossental, Jaufen Pass).

amphibolites. These pre-Hercynian para and orthorocks of the Basement are cut by younger post-Hercynian diabase dikes.

Geochemical investigations of amphibolites from the Oetztal-Stubai complex (MOGESSIE, 1984; MOGESSIE et al., 1985) show striking regional differences from N/NW to S/SE. Major and trace element chemistry data indicate a typical magmatic trend (ortho-amphibolite) for amphibolites of central and N/NW Oetztal (originated from a tholeiitic magma) whereas amphibolites from S/SE Oetztal (Schneeberg complex) were found to be para-amphibolites.

Based on petrological studies of the metapelites (PURTSCHELLER, 1967, 1969; HOINKES, 1981); the metabasites (MILLER, 1970; HOERNES & HOFFER, 1973; PURTSCHELLER & RAMMLMAIR, 1981), the carbonate rocks (HOINKES, 1978; 1983), the granitoids (HOINKES et al., 1972), radiometric investigations (THÖNI, 1980, 1981) and as recently summerized by HOINKES et al. (1982) the Oetztal-Stubai complex is considered to be an example of an overprint by two successive metamorphic events, which now appear as heat domes of similar grade, but geographically separated by a distance of 35 km.

The dominant metamorphism is of Hercynian age and reached a maximum temperature of 670°C (Winnebach migmatite). It is important to note that SÖLLNER & SCHMIDT (1981) have determined a Caledonian age of 463±37 m.y. for this migmatite, which is at the moment controversial. This heat dome is overprinted by a later cretaceous metamorphism with a temperature climax of about 600°C in the south (south of Schneeberger Zug). The metamorphic grade of this younger event and its retrograde effect on the pre-Alpine parageneses decreases to the northwest (see Fig. 1: Hercynian mica cooling ages, alpine biotite cooling ages, zone of mixed ages of THÖNI [1981], and Alpine chloritoid line by PURTSCHELLER [1967]).

2. Petrography

2.1. Amphibolite

The amphibolite assemblage mostly consists of elongate, parallel crystals of colourless, blue-green to brown hornblendes; epidote, plagioclase, biotite, chlorite with subordinate amounts of quartz, carbonate, sphene, rutile and ilmenite. In some samples all the three common titanium oxides are present, generally displaying a replacement texture rutile-ilmenite-sphene. Hornblende ranges from 30 % to 65 % by volume. The hornblendes are mostly zoned with distinct sharp optical boundary. The zoning is characterized by a colourless, very weakly pleochroic actinolite core and a greenish hornblende rim in one case (samples MK-3, KN-1, ASC-2) and a greenish hornblende core with a colourless actinolite rim in the other (samples RL, L-37, LT-126, MK-8, DO-417). In some samples Fe-Mg amphiboles occur. Cummingtonite grows with calcic amphibole actually sharing the same crystallographic boundary, and in some cases the colourless cummingtonite rims greenish hornblende. Anthophyllite lamellae in calcic amphibole associated with talc-chlorite-actinolite also occur in only one sample from Pollestal (PA-42). These parageneses mostly occur at grain boundaries and textural evidence suggests a retrograde process.

Plagioclase feldspars range from 10 % to 30 % by volume. Twinning is rarely observed. Albite occurs as single grain (e. g. ASC-1 from Pfossental) and as a retrograde product (e. g. DO-417 from Kühtai). Some grains are intensively sericitized and altered to aggregates of clinozoisite and white mica (e. g. FL-1 & FL-2 from Fotschertal). Alkali feldspars have been observed only in very few samples (e. g. KN-5 from Kaunertal, and S-10 from Burgstein) as secondary alteration product.

Epidote-clinozoisite minerals occur as granular or crudely tabular forms associated with hornblende and plagioclase. Some samples contain up to 30 % epidote by volume. In most cases the epidotes are zoned.

Biotite and chlorite occur as primary phases and as retrograde products of hornblende. Chlorites that have been produced as a result of a retrograde process from hornblende show anomalous interference colour.

2.2. Garnet amphibolite

Generally considered the garnet amphibolites can be characterized by 47–49 % hornblende, 28–30 % plagioclase, 3–10 % garnet, 0,2–13 % biotite, 0–1 % chlorite, 0–3 % epidote, 2–4 % quartz, 1–2 % sphene and 2–5 % ilmenite in modal abundance. The garnets are euhedral to anhedral in shape with varying grain size. The garnets and hornblendes commonly alter to chlorite; and this is more pronounced in garnet amphibolites of southeastern Oetztal. Some garnets are optically zoned mostly with inclusion rich cores (quartz, epidote) and inclusion free homogenous rims. The hornblendes display varying textures and colour (ranging from colourless to greenish/brown).

2.3. Eclogite amphibolite

Microscopically these rock series are characterized by garnet grains of varying grainsize within a feldspar-plagioclase matrix and some relics of the original omphacite; and one observes the formation of greenish hornblende around garnet and homogenization of the matrix, where the pyroxene and garnet are being replaced by hornblende and plagioclase. The garnets have inclusions of rutile, hornblende and in rare cases kyanite and quartz.

2.4. Diablastic garnet amphibolite

The diablastic garnet amphibolites are characterized by the formation of more diablasts (feldspars and hornblende) and zoisite from the primary mineral parageneses clinopyroxene, colourless hornblende, garnet and kyanite.

The garnet rim contains hornblende, plagioclase and titanium oxides such as ilmenite. Quartz occurs scattered in the matrix. Kyanite totally alters to zoisite.

3. Analytical methods and data reduction

Chemical compositions of minerals were analysed with an ARL-SEMQ electronmicroprobe at the Institute

of Mineralogy and Petrography University of Innsbruck using standard methods. The matrix effects were corrected according to BENCE & ALBEE (1968).

Each mineral was subjected to several spot analyses depending on the size of the grain. Where significant zoning was found, such as in amphibole, epidote, plagioclase and garnet, analytical data are presented for core and rim compositions in the respective tables. Where variation in composition for each phase is found to be significant such as the calcic amphiboles, averages are given.

Electronmicroprobe technique does not allow for routine distinction of Fe^{2+} and Fe^{3+}; therefore, total iron was considered as Fe^{2+} in chlorite, biotite, garnet, and Fe^{3+} in plagioclase and epidote. For amphiboles the minimum and maximum amount of Fe^{3+} that could be present in an amphibole structure of a given chemistry was calculated and an attempt has been made to determine the name based on amphibole nomenclature of LEAKE (1978). Cation proportions were calculated on anhydrous basis.

4. Mineral chemistry

4.1. Plagioclase

Plagioclase from most of the garnet-bearing and garnet-free amphibolites have been analysed and show a wide range of compositions. Representative analyses are presented in Table 1.

Eventhough correlation of plagioclase composition with specific metamorphic stages is difficult because of the obscuring overprint resulting from the polymetamorphic nature of the region, a general picture of variation in An-content can be pointed out. The presence of pure albite in sample ASC-1 from Pfossental, and a feldspar compositon of An_{10} from a nearby sample, with a trend of increasing An-content towards central Schneeberger Zug (reaching a maximum value of An_{60} in a garnet amphibolite from Seebertal), suggests that around the Eishof the Alpine amphibolite facies grades into a lower grade greenschist facies. In most cases the presence of albite rimming An-rich core occurs in the same region where actinolite is found rimming Al-rich hornblende core (see Fig. 1: locations 4, 5, 6, 9 & 11). This suggests a retrograde phenomenon from amphibolite to greenschist facies.

Alternatively, the majority of the analysed plagioclase grains show inverse zonation with An-poor core and An-rich rim.

The general rise in An-content is associated with decline of modal epidote and increase in the alumina content of amphibole. This is the prograde metamorphic effect that has been documented by several authors (LEAKE, 1965; LIOU et al., 1974; SPEAR, 1981; LAIRD & ALBEE, 1981).

4.2. Amphiboles

Electronmicroprobe analyses of the amphiboles from the Oetztal-Stubai amphibolites are presented in Table 2.

Various procedures have been proposed for calculating amphibole analyses (HIMMELBERG & PAPIKE, 1969; ROBINSON, ROSS & JAFFE, 1971). In the present case the method proposed by STOUT (1972) to calculate the maximum and minimum amount of Fe^{3+} in an amphibole structure based on stochiometric constraints is employed. The analytical data of the amphiboles are reduced by a computer program designed specifically for

Table 1: Representative Electronmicroprobe analyses of feldspars from the amphibolites of the Oetztal-Stubai Basement.

	ASC-1	SW-185	S-9	PA-4	PZ-5	KN-6	DO-417/1	DO-417/2
SiO_2	67.81	53.34	59.08	63.45	62.29	59.04	57.37	68.40
TiO_2	0.00	0.00	0.00	0.00	0.00	0.00	0.00	0.07
Al_2O_3	20.09	28.00	25.54	24.64	23.32	25.88	27.44	20.87
FeO	0.20	0.19	0.33	0.33	0.14	0.08	0.35	0.39
MnO	0.00	0.00	0.00	0.02	0.00	0.00	0.00	0.00
MgO	0.01	0.26	0.05	0.04	0.01	0.00	0.00	0.21
CaO	0.21	12.65	7.39	4.82	4.31	6.92	8.87	0.44
K_2O	0.07	0.07	0.09	0.10	0.08	0.06	0.09	0.16
Na_2O	11.33	4.67	6.99	7.14	8.60	7.56	6.61	9.21
Total	99.72	99.18	99.47	100.54	98.75	99.54	100.73	99.75
	Atoms per formula unit based on 8 Oxygens							
Si	2.9713	2.4405	2.6491	2.7743	2.7848	2.6434	2.5567	2.9748
Al	1.0375	1.5099	1.3497	1.2698	1.2287	1.3656	1.4413	1.0698
Ti	0.0000	0.0000	0.0000	0.0000	0.0000	0.0000	0.0000	0.0023
Fe	0.0073	0.0073	0.0124	0.0121	0.0052	0.0030	0.0130	0.0142
Mn	0.0000	0.0000	0.0000	0.0007	0.0000	0.0000	0.0000	0.0000
Mg	0.0007	0.0177	0.0033	0.0026	0.0007	0.0000	0.0000	0.0136
Ca	0.0099	0.6201	0.3550	0.2258	0.2064	0.3320	0.4235	0.0205
K	0.0039	0.0041	0.0051	0.0056	0.0046	0.0034	0.0051	0.0089
Na	0.9626	0.4143	0.6077	0.6053	0.7455	0.6563	0.5711	0.7766
Total	4.9932	5.0139	4.9823	4.8962	4.9759	5.0037	5.0107	4.8807
Or	0.40	0.39	0.53	0.67	0.48	0.35	0.51	1.10
Ab	98.59	39.89	62.79	72.35	77.94	66.18	57.13	96.35
An	1.01	59.71	36.68	26.99	21.58	33.48	42.36	2.54

Table 2: Representative Electronmicroprobe analyses of calcic amphiboles from the amphibolites of the Oetztal-Stubai Basement.

	PZ-1	PZ-2	PZ-4	PZ-5	KN-5	KN-6	ST-3	N494
SiO_2	45.77	42.21	42.06	44.56	45.71	43.67	48.08	45.79
TiO_2	0.44	0.74	0.76	0.67	0.72	0.81	0.63	0.44
Al_2O_3	13.50	13.82	12.40	11.94	9.18	11.92	8.84	11.66
FeO	12.96	18.66	17.32	15.37	17.52	16.42	13.27	14.77
MnO	0.22	0.37	0.28	0.39	0.28	0.42	0.43	0.27
MgO	11.99	8.32	10.27	11.80	10.79	11.08	12.76	11.55
CaO	10.85	10.36	12.48	11.21	13.09	12.26	12.67	11.72
K_2O	0.20	0.53	0.37	0.27	0.19	0.62	0.35	0.54
Na_2O	1.76	2.16	1.82	1.80	1.23	1.53	0.93	1.67
Total	97.69	97.17	97.76	98.01	98.71	98.73	97.96	98.41
	Atoms per formula unit based on 23 oxygens and $Fe_{Total}=Fe^{2+}$							
Si	6.6448	6.3944	6.3395	6.5721	6.7806	6.4693	6.9890	6.7006
Al^{IV}	1.3552	1.6056	1.6605	1.4279	1.2194	1.5307	1.0110	1.2994
Al^{VI}	0.9547	0.8619	0.5423	0.6477	0.3855	0.5505	0.5035	0.7116
Ti	0.0485	0.0852	0.0870	0.0751	0.0811	0.0912	0.0917	0.0489
Fe	1.5734	2.3640	2.1831	1.8957	2.1734	2.0342	1.6131	1.8075
Mn	0.0271	0.0475	0.0357	0.0487	0.0352	0.0527	0.0529	0.0335
Mg	2.5940	1.8783	2.3068	2.5936	2.3852	2.4461	2.7641	2.5187
Ca	1.6877	1.6815	2.0154	1.7715	2.0805	1.9459	1.9733	1.8375
Na	0.4954	0.6344	0.5319	0.5147	0.3538	0.4395	0.2621	0.4738
K	0.0370	0.1024	0.0711	0.0508	0.0360	0.1172	0.0649	0.1008
Total	15.4178	15.6552	15.7733	15.5978	15.5307	15.6773	15.3256	15.5323
	Magnesio-Hornblende	Tschermakitic-Hornblende	Magnesian-Hastingsite-Hornblende	Tschermakitic-Hornblende	Magnesio-Hornblende	Tschermakitic Hornblende	Magnesio-Hornblende	Magnesio-Hornblende

	PA-3	PA-4	MK-1	MK-3	MK-8	S6	S9	S10
SiO_2	44.37	43.92	46.21	40.02	45.86	43.06	42.71	44.10
TiO_2	0.48	0.80	0.44	0.26	0.21	0.27	0.72	0.46
Al_2O_3	13.03	11.29	12.07	14.58	12.25	15.21	13.04	9.87
FeO	15.56	17.56	12.68	12.44	11.07	14.71	14.83	17.11
MnO	0.11	0.41	0.26	0.24	0.20	0.22	0.31	0.18
MgO	11.55	9.73	12.96	13.23	14.18	10.52	11.36	11.01
CaO	11.28	11.92	12.26	12.84	12.24	11.34	12.52	12.63
K_2O	0.11	0.59	0.34	0.24	0.18	0.20	0.35	0.35
Na_2O	2.41	1.72	1.70	2.37	1.46	2.10	1.93	1.45
Total	98.90	97.94	98.92	96.22	97.65	97.63	97.77	97.16
	Atoms per formula unit based on 23 Oxygens and $Fe_{Total}=Fe^{2+}$							
Si	6.4871	6.5868	6.6608	6.0263	6.6381	6.3527	6.3512	6.6565
Al^{IV}	1.5129	1.4132	1.3392	1.9737	1.3619	1.6473	1.6488	1.3435
Al^{VI}	0.7323	0.5823	0.7113	0.6138	0.7279	0.9974	0.6366	0.4123
Ti	0.0533	0.0912	0.0482	0.0297	0.0231	0.0303	0.0813	0.0528
Fe	1.9024	2.2023	1.5285	1.5665	1.3400	1.8149	1.8442	2.1597
Mn	0.0136	0.0521	0.0317	0.0306	0.0245	0.0275	0.0390	0.0230
Mg	2.5165	2.1746	2.7839	2.9689	3.0587	2.3129	2.5174	2.4766
Ca	1.7670	1.9154	1.8934	2.0716	1.8983	1.7925	1.9948	2.0426
Na	0.6832	0.5001	0.4751	0.6919	0.4097	0.6007	0.5565	0.4244
K	0.0205	0.1129	0.0625	0.0461	0.0332	0.0376	0.0664	0.0674
Total	15.6888	15.6309	15.5346	16.0191	15.5154	15.6138	15.7362	15.6588
	Tschermakitic-Hornblende	Edenitic-Hornblende	Magnesio-Hornblende	Magnesio-Hornblende	Magnesio-Hornblende	Tschermakitic-Hornblende	Ferroan-Pargasitic Hornblende	Edenitic-Hornblende

Table 2 (continued).

	WSC-1	WSC-2	P-21	SW-185	RL	FL-1	G-2	VN-1
SiO_2	46.66	43.20	43.05	43.60	48.99	43.55	43.49	42.86
TiO_2	0.51	0.62	0.51	0.57	0.34	0.73	0.54	0.53
Al_2O_3	13.11	12.46	14.89	15.74	11.86	14.42	14.18	14.27
FeO	13.02	18.91	14.97	14.28	12.32	14.91	17.00	15.82
MnO	0.23	0.18	0.20	0.07	0.20	0.24	0.21	0.31
MgO	11.94	9.16	10.83	10.91	13.58	10.76	9.31	9.10
CaO	10.99	9.35	11.87	11.53	9.69	12.24	10.11	11.71
K_2O	0.39	0.41	0.40	0.44	0.24	0.46	0.60	0.50
Na_2O	1.62	1.76	1.46	1.50	1.28	1.51	1.90	1.57
	98.47	96.05	98.18	98.64	98.50	98.82	97.34	96.67
	Atoms per formula unit based on 23 Oxygens and $Fe_{Total}=Fe^{2+}$							
Si	6.7183	6.5805	6.3303	6.3372	6.9575	6.3685	6.4871	6.4348
Al^{IV}	1.2817	1.4195	1.6697	1.6628	1.0425	1.6315	1.5129	1.5652
Al^{VI}	0.9429	0.8174	0.9108	1.0335	0.9427	0.8539	0.9799	0.9599
Ti	0.0558	0.0718	0.0570	0.0629	0.0367	0.0811	0.0619	0.0605
Fe	1.5677	2.4089	1.8408	1.7357	1.4632	1.8234	2.1206	1.9863
Mn	0.0280	0.0232	0.0249	0.0086	0.0241	0.0297	0.0265	0.0394
Mg	2.5619	2.0793	2.3732	2.3631	2.8741	2.3449	2.0695	2.0360
Ca	1.6954	1.5260	1.8701	1.7956	1.4745	1.9178	1.6158	1.8837
Na	0.3522	0.5257	0.4163	0.4227	0.3525	0.4281	0.5495	0.4570
K	0.0716	0.0797	0.0750	0.0816	0.0435	0.0858	0.1142	0.0958
Total	15.2755	15.5320	15.5681	15.5037	15.2113	15.5647	15.5379	15.5186
	Magnesio-Hornblende	Tschermakitic-Hornblende	Tschermakite	Tschermakite	Magnesio-Hornblende	Tschermakitic-Hornblende	Tschermakitic-Hornblende	Tschermakitic Hornblende

Table 3: Representative Electronmicroprobe analyses of zoned calcic amphiboles from the amphibolites of the Oetztal-Stubai Basement.

	KN-1		PZ-3		MK-3		ASC-2	
	core	rim	core	rim	core	rim	core	rim
SiO_2	53.52	43.84	50.63	44.52	52.98	43.30	51.39	47.29
TiO_2	0.09	0.31	0.23	0.74	0.05	0.40	0.22	0.44
Al_2O_3	3.10	13.79	8.58	12.19	3.53	12.60	6.54	11.42
FeO	9.74	13.47	7.36	8.87	7.17	12.87	11.10	12.74
MnO	0.20	0.18	0.14	0.20	0.03	0.21	0.17	0.24
MgO	18.12	14.42	16.88	15.81	19.29	12.95	14.46	11.64
CaO	13.28	9.82	11.45	12.92	13.64	13.06	11.20	10.42
K_2O	0.08	0.43	0.15	0.28	0.08	0.10	0.17	0.27
Na_2O	0.33	0.71	1.26	1.79	0.54	2.17	1.06	1.77
Total	98.46	96.97	96.68	97.32	97.31	97.66	96.31	96.23
	Atoms per formula unit based on 23 Oxygens and $Fe_{Total}=Fe^{2+}$							
Si	7.5763	6.4223	7.1938	6.4554	7.5017	6.3805	7.4359	6.9272
Al^{IV}	0.4237	1.5777	0.8062	1.5446	0.4983	1.6195	0.5641	1.0728
Al^{VI}	0.0916	0.8032	0.6306	0.5387	0.0908	0.5688	0.5512	0.8988
Ti	0.0096	0.0345	0.0248	0.0815	0.0054	0.0448	0.0242	0.0490
Fe	1.1488	1.6502	0.8745	1.0756	0.8490	1.5860	1.3432	1.5606
Mn	0.0239	0.0233	0.0168	0.0246	0.0036	0.0262	0.0208	0.0298
Mg	3.8084	3.1480	3.5742	3.4163	4.0704	2.8438	3.1180	2.5410
Ca	2.0067	1.5410	1.7431	2.0072	2.0693	2.0619	1.7364	1.6354
Na	0.0902	0.2017	0.3471	0.5032	0.1482	0.6200	0.2974	0.5027
K	0.0144	0.0804	0.0272	0.0518	0.0145	0.0188	0.0314	0.0505
Total	15.1936	15.4823	15.2383	15.6989	152512	15.7703	15.1226	15.2678
	Actinolite	Tschermakite	Magnesio-Hornblende	Magnesio-Hastingsite-Hornblende	Actinolite	Ferroan-Pargasitic-Hornblende	Actinolitic-Hornblende	Magnesio-Hornblende

Table 3 (continued).

	MK-8		PA-4		RL		LT-126	
	core	rim	core	rim	core	rim	core	rim
SiO_2	44.76	54.92	43.92	52.55	48.99	53.83	45.54	54.23
TiO_2	0.58	0.02	0.80	0.06	0.34	0.11	0.42	0.18
Al_2O_3	12.99	3.63	11.29	2.22	11.86	3.41	12.73	3.70
FeO	12.01	8.11	17.56	16.67	12.32	8.85	11.63	8.11
MnO	0.20	0.15	0.41	0.31	0.20	0.16	0.14	0.11
MgO	12.96	18.45	9.73	12.80	13.58	19.10	13.15	18.26
CaO	12.75	13.33	11.92	12.92	9.69	12.21	11.42	12.17
K_2O	0.56	0.03	0.59	0.17	0.24	0.03	0.24	0.01
Na_2O	1.75	0.28	1.72	0.20	1.28	0.29	1.78	0.59
Total	98.56	98.92	97.94	97.90	98.50	97.99	97.05	97.36
	Atoms per formula unit based on 23 Oxygens and $Fe_{Total}=Fe^{2+}$							
Si	6.4869	7.6383	6.5838	7.7162	6.9575	7.5846	6.6385	7.6520
Al^{IV}	1.5131	0.3617	1.4162	0.2838	1.0425	0.4154	1.3615	0.3480
Al^{VI}	0.7057	0.2333	0.5785	0.1004	0.9427	0.1508	0.8256	0.2673
Ti	0.0639	0.0021	0.0911	0.0067	0.0367	0.0118	0.0465	0.0193
Fe	1.4556	0.9433	2.2013	2.0470	1.4632	1.0428	1.4178	0.9570
Mn	0.0246	0.0177	0.0521	0.0386	0.0241	0.0191	0.0173	0.0131
Mg	2.7990	3.8240	2.1736	2.8009	2.8741	4.0105	2.8567	3.8397
Ca	1.9798	1.9864	1.9145	2.0326	1.4745	1.8433	1.7837	1.8399
Na	0.4917	0.0755	0.4999	0.0569	0.3525	0.0792	0.5031	0.1614
K	0.1035	0.0053	0.1128	0.0318	0.0435	0.0054	0.0446	0.0018
Total	15.6238	15.0576	15.6238	15.1149	15.2113	15.1629	15.4953	15.0995
	Actinolite	Ferroan-Pargasitic-Hornblende	Actinolite	Edenitic-Hornblende	Tremolitic-Hornblende	Magnesio-Hornblende	Actinolite	Magnesio-Hornblende

amphiboles (MOGESSIE & TESSARDI, 1982), following the recommendation of the IMA nomenclature compiled by LEAKE (1978).

The calculated structural formulae of the amphiboles (Tables 2 & 3) indicate that at least some coupled substitution mechanisms (SPEAR, 1981) were operative in the Oetztal-Stubai amphiboles.

On Figs. 2 a,b the NW Oetztal (Pitztal, Kaunertal) amphiboles plot above the pargasite substitution line and towards the edenite substitution, indicating an edenite-ferro-edenite composition resulting from a tremolite composition by the entry of Na into the A-site together with a balancing replacement of one Si by one Al:

$$Na^{A}Al^{IV} = Si^{IV} \quad (1)$$

The samples from the SE Oetztal plot towards tschermakite, actually reflecting a tschermakite-ferro-tschermakite substitution derived from a tremolite composition by the substitution of the following type:

$$Al^{VI}Al^{IV} = Mg^{VI}Si^{IV} \quad (2)$$

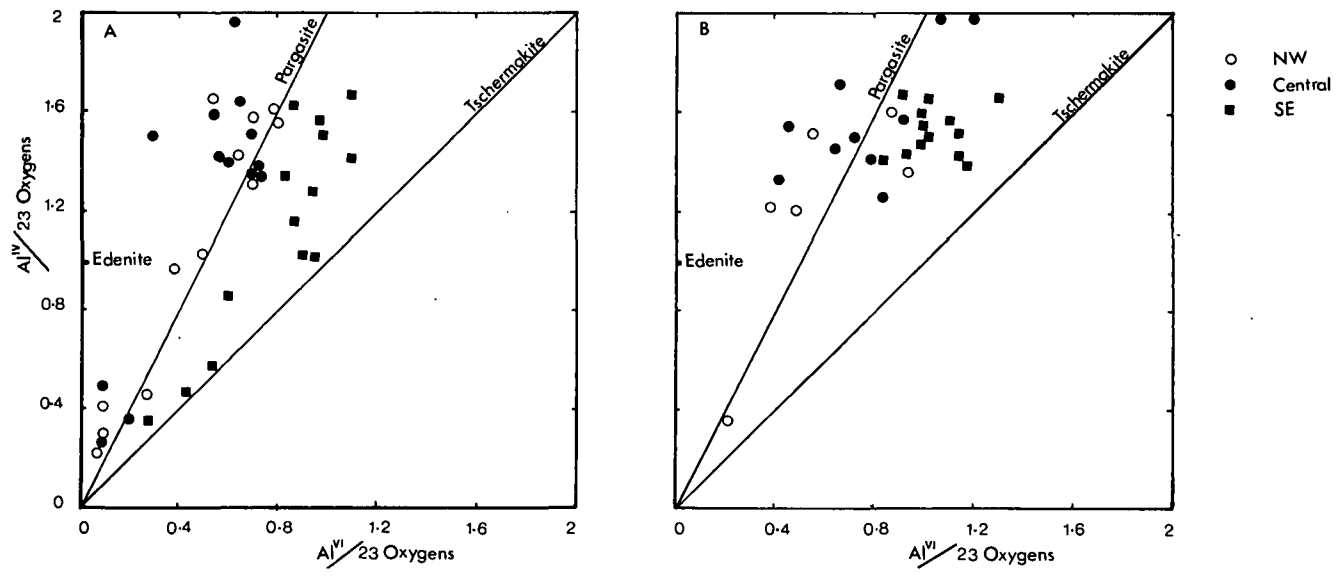

Fig. 2: Plot of Al^{IV} vs. Al^{VI} for calcic amphiboles from the amphibolites of the Oetztal-Stubai Basement. Open circles: N/NW Oetztal; closed circles: Central Oetztal; closed squares: SE Oetztal.

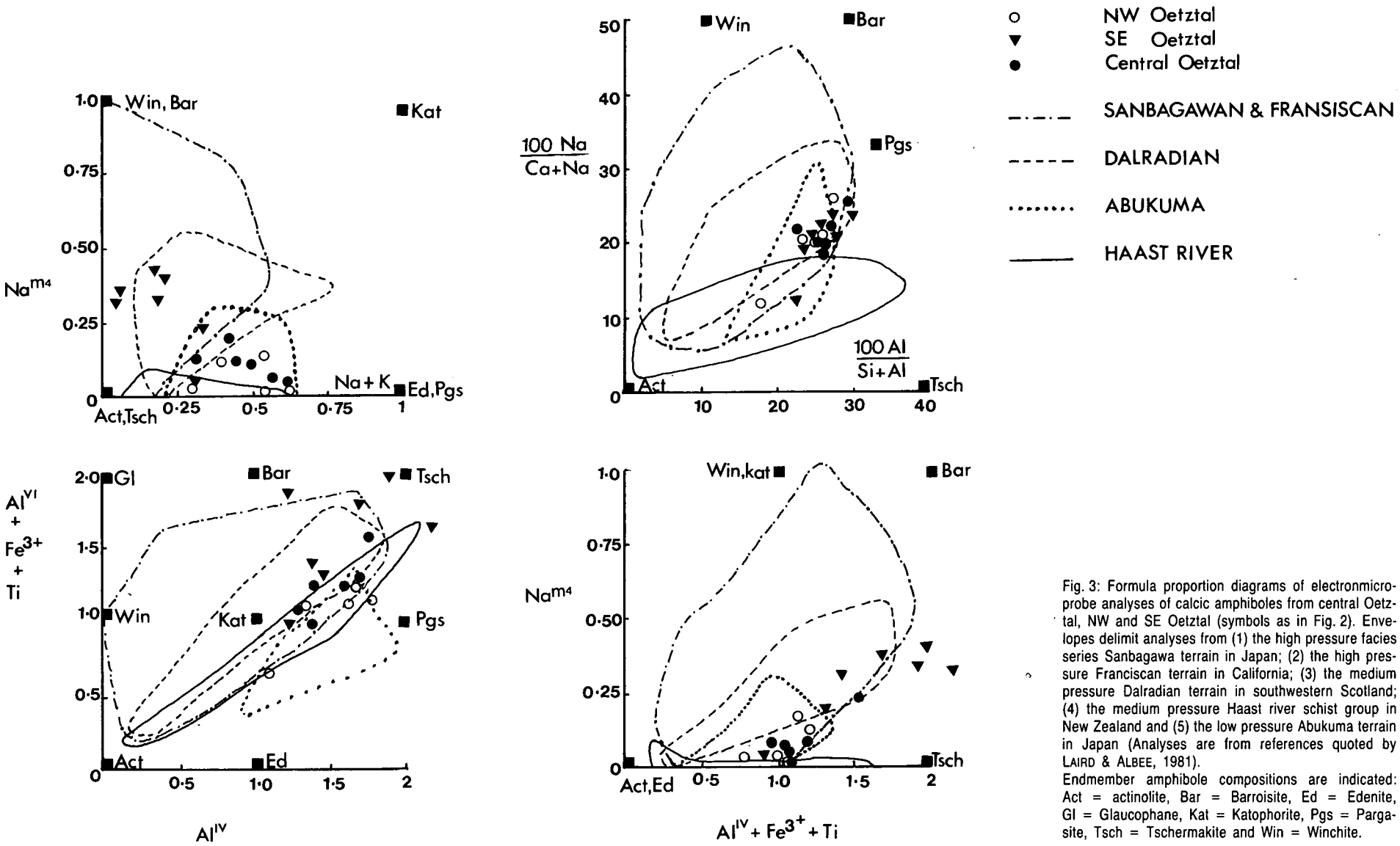

Fig. 3: Formula proportion diagrams of electronmicroprobe analyses of calcic amphiboles from central Oetztal, NW and SE Oetztal (symbols as in Fig. 2). Envelopes delimit analyses from (1) the high pressure facies series Sanbagawa terrain in Japan; (2) the high pressure Franciscan terrain in California; (3) the medium pressure Dalradian terrain in southwestern Scotland; (4) the medium pressure Haast river schist group in New Zealand and (5) the low pressure Abukuma terrain in Japan (Analyses are from references quoted by LAIRD & ALBEE, 1981).
Endmember amphibole compositions are indicated: Act = actinolite, Bar = Barroisite, Ed = Edenite, Gl = Glaucophane, Kat = Katophorite, Pgs = Pargasite, Tsch = Tschermakite and Win = Winchite.

The central Oetztal (Sölden–Längenfeld) samples plot below and on the pargasite substitution line. This type of substitution is produced by a combination of the edenite and tschermakite substitutions indicated in (1) and (2) above:

$$Na^{A}Al^{IV} + Al^{VI}Al^{IV} = Mg^{VI}Si^{IV} + Si^{IV}$$
$$NaAl_3 = MgSi_2$$

Figures 3 and 4 show that the calcic amphiboles of the Oetztal-Stubai Basement plot in an area bounded by the endmembers tschermakite and edenite. The plot of Al^{IV} vs. Na+K for the Oetztal amphiboles is similar to the plots of HIETANEN (1974) and JAN & HOWIE (1982) with the ratio at about 3 : 1.

As can be seen in Figs. 3 a,b and c where boundaries are indicated for amphiboles of the high pressure Sanbagawa and Fransiscan terrain, the medium pressure of the Dalradian and the low pressure fields of the Abukuma plateau and the Haast river; the Oetztal-Stubai, especially the central and NW Oetztal amphiboles, plot within the overlapping region of the Sanbagawa and Fransiscan terrain, the Dalradian and Abukuma plateau. This suggests changing pressure conditions from low to medium pressure within the Oetztal-Stubai Basement. The amphiboles from the southeast are scattered in all the plots but indicate a trend towards medium pressure conditions.

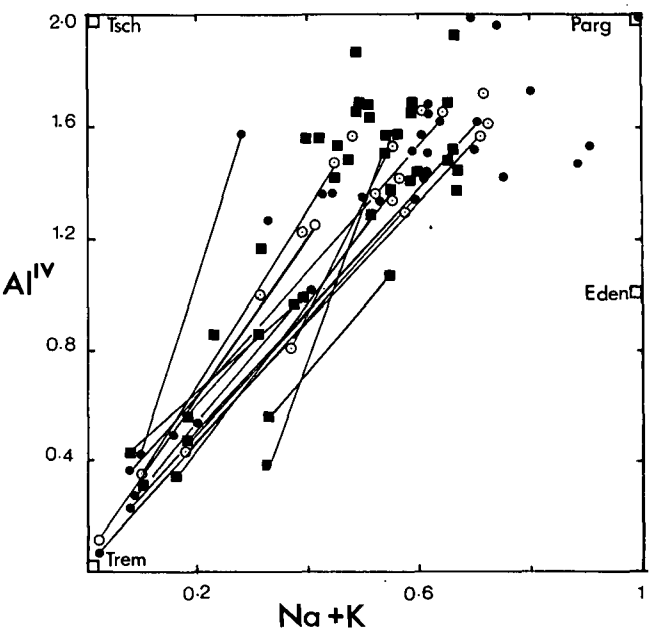

Fig. 4: Al^{IV} vs. (Na+K) plot for calcic amphibole analyses. Tielines indicate core and rim compositions of zoned calcic amphiboles. Symbols as in Fig. 2.

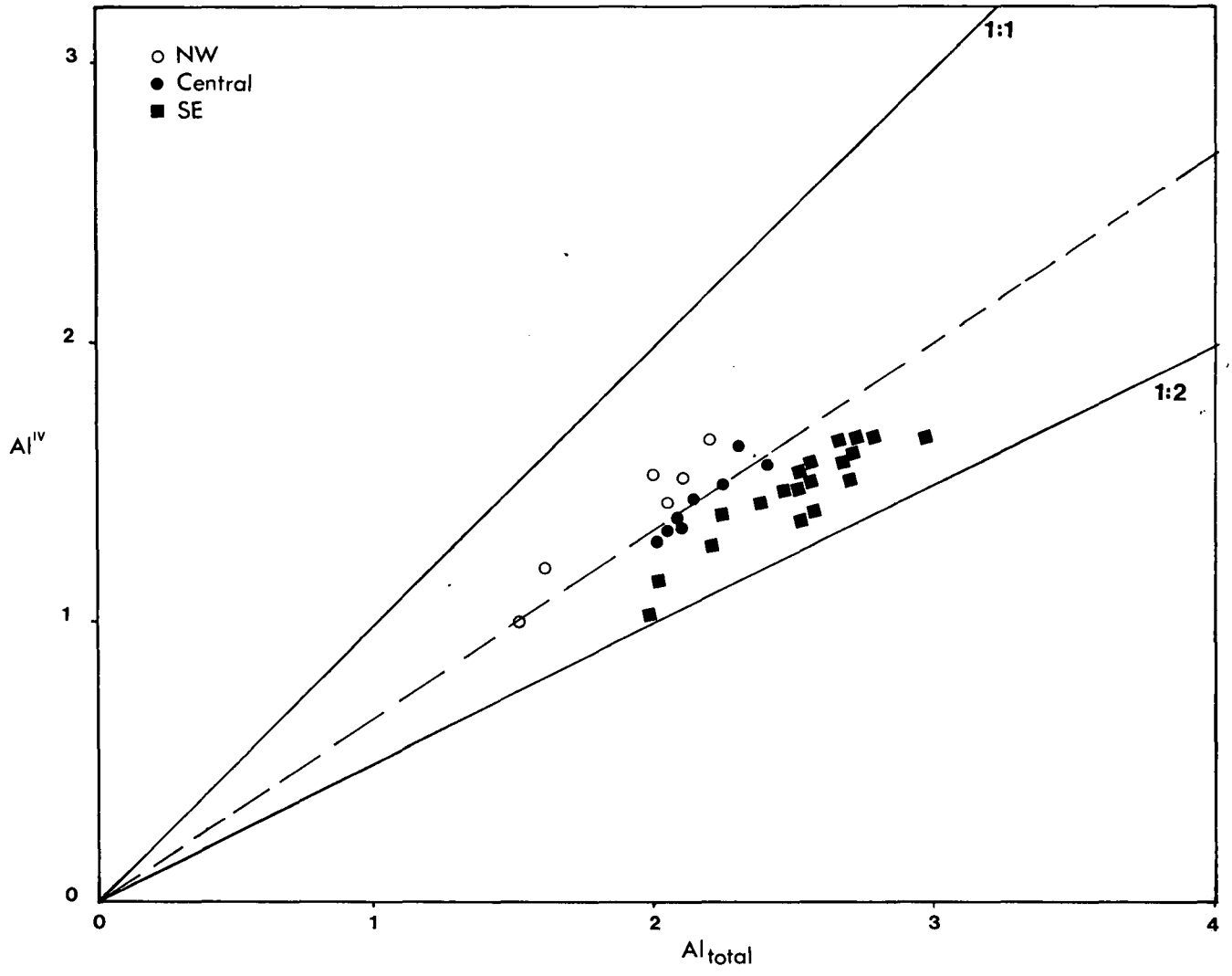

Fig. 5: Al_{total} vs. Al^{IV} plot of calcic amphiboles from the regionally distributed amphibolites of the Oetztal-Stubai Basement. Symbols as in Fig. 2.

Apart from the low alumina calcic amphiboles (actinolites), the majority of the calcic amphiboles are characterized by more than half-filled A-site (i. e. >0,5, Fig. 4).

Considering the Ti-content of the calcic amphiboles a higher value (Ti = 0,88) from the NW Oetztal and a lower value (Ti = 0,04) in the central Oetztal, especially amphiboles from eclogite or diablastic garnet amphibolites is registered. This same regional difference is also displayed by the Al^{IV} vs. Al_{total} plot (Fig. 5) whereby the amphiboles from the NW and central Oetztal occupy a region around the 1 : 1 line and those from the SE plot in a region with a ratio $Al^{IV} : Al_{total}$ close to 1 : 2, indicating a higher grade of metamorphism in central and NW Oetztal compared to those in the SE (MISCH & RICE, 1974).

4.2.1. Hornblende actinolite series

The Oetztal-Stubai amphibolites are marked by hornblendes of varying textures and chemical inhomogeneity. Zoned calcic amphiboles of colourless actinolite core, greenish hornblende rim and vice versa are observed in several amphibolite samples. The sharp optical discontinuity is also marked by a similar discontinuity in chemistry (Table 3).

In most studies of the actinolite-hornblende series in calcic amphiboles the gap in chemistry between the Al-rich and Al-poor end members is considered to be due to the presence of miscibility gap between tremolite/actinolite and hornblende (HALLIMOND, 1943, KLEIN, 1969; COOPER & LOVERING, 1970; DOOLAN et al., 1973; BRADY, 1974; KUNIYOSHI & LIOU, 1976); and due to abrupt change (or discontinuous change) in the composition of, or in the appearance or disappearance of, other phases involved in reactions occurring at the actinolite-hornblende transition (SMULIKOWSKI, 1974; COMPTON, 1958; GRAHAM, 1974; GRAPES, 1975; GRAPES & GRAHAM, 1978).

The question of the presence of a miscibility gap or a disequilibrium reaction are considered below. Evidence cited by most authors (references quoted above) for supposed equilibrium crystallization, and therefore the existence of a miscibility gap between actinolite and hornblende include:

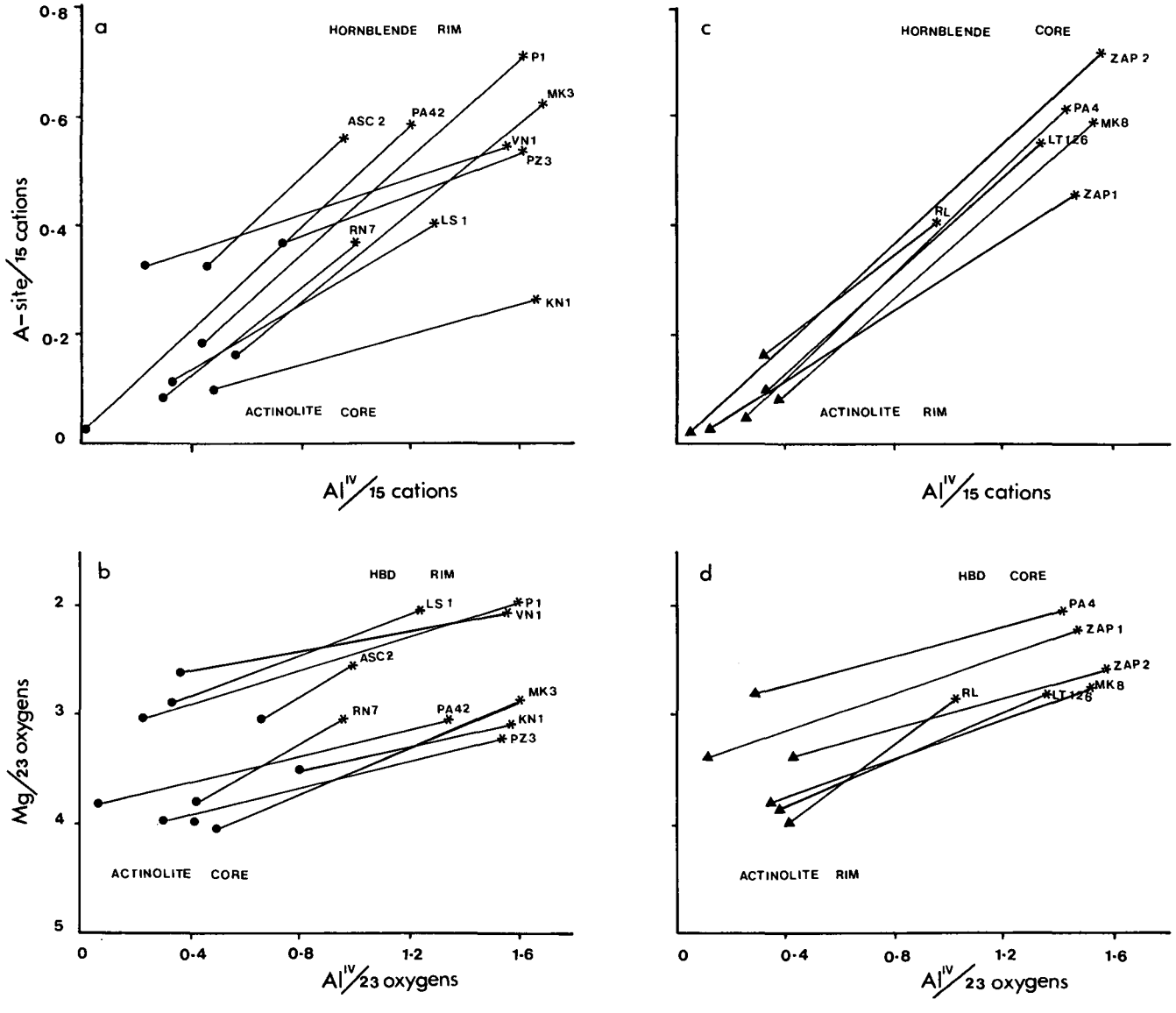

Fig. 6: A-site vs. Al^{IV}(a&c) and Mg. vs. Al^{IV}(b&d) plots of zoned calcic amphiboles from the Oetztal-Stubai amphibolites. a and b indicate core and rim compositions of Hercynian calcic amphiboles. c and d represent hornblende core of Hercynian age and actinolite rim of Alpine overprint.

1. The large chemical difference and composition gaps between actinolite and hornblende in various terrains.
2. Sharp contacts, both optically and chemically between actinolite and hornblende; hornblende typically rims actinolite in a simple zonal arrangement, and/or occurs as an irregular patchy domain within actinolite.
3. Separate, homogenous grains or fibers of the two amphiboles.
4. Exsolution lamellae of hornblende in actinolite and vice versa.

If petrographically observed, only evidence of types (3) or (4) are in themselves believed to be sufficient to establish the existence of a miscibility gap.

The actinolite-hornblende series of the Oetztal-Stubai amphibolites are characterized by (1) and (2) given above. Sample KN-1 from Kaunertal and sample MK-3 from Milchenkar show large actinolite cores with numerous lamellae parallel to the cleavage surfaces and greenish hornblende rim free from these lamellae. Since the lamellae are very small a painstaking effort has been made to check their chemistry with the electronmicroprobe and an attached energy dispersive system. To our surprise these lamellae (especially those from Kaunertal) proved to be epidote, quartz, and chlorite inclusions rather than a hornblende lamellae in actinolite.

Therefore, this evidence suggests the presence of relict low grade greenschist mineral paragenesis which have been preserved as a result of a disequilibrium or discontinuous reaction which caused an abrupt change from colourless actinolite to greenish hornblende of high alumina content.

The actinolite-hornblende transition can be defined by several reactions accompanied with complex changes associated with the breakdown or compositional change of albite to oligoclase, chlorite becomes more magnesium rich and ultimately disappears. These changes in chemistry and final disappearance of some phases (chlorite, epidote) with increasing grade of metamorphism contribute to the production of hornblende from actinolite according to the generalized reactions suggested by (SHIDO, 1958; COOPER, 1972; LIOU et al., 1974; GRAHAM, 1974) and outlined below.

❶ $NaAlSi_3O_8$ (albite) + $Ca_2(Mg,Fe)_5Si_8O_{22}(OH)_2$ (trem/actinolite) = $NaCa_2(Mg,Fe)_5AlSi_7O_{22}(OH)_2$ (edenite) + 4 SiO_2 (quartz)

❷ $Ca_2(Mg,Fe)_5Si_8O_{22}(OH)_2$ (trem/actinoilite) + + 14 $(Mg,Fe)_5Al_2Si_3O_{10}(OH)_8$ (clorite) + + 24 $Ca_2Al_3Si_3O_{12}(OH)$ (epidote) + 28 SiO_2 (quartz) = 25 $Ca_2(Mg,Fe)_3Al_4Si_6O_{22}(OH)_2$ (tschermakite) + + 44 H_2O

❸ 6 $(Mg,Fe)_5Al_2Si_3O_{22}(OH)_8$ (chlorite) + + 12 $Ca_2Al_3Si_3O_{12}(OH)$ (epidote) + 14 SiO_2 (quartz) = 10 $Ca_2(Mg,Fe)_3Al_4Si_6O_{22}(OH)_2$ (tschermakite) + + 4 $CaAl_2Si_2O_8$ (anorthite) + $20H_2O$.

Reaction ❶ is dominant in NW Oetztal where at high temperature and low pressure the edenite substitution becomes dominant (Fig. 2). In SE Oetztal the tschermakite substitution is dominant and the central Oetztal is represented by calcic amphibole series displaying pargasite type substitution.

Thus the central and SE Oetztal actinolite-hornblende transition are dominated by reactions ❷ and ❸. This combination of the edenite and tschermakite substitutions results (as also outlined above) in a decrease or disappearence of epidote thereby increasing the Al-content of the plagioclase; enrichment of chlorite in Mg with increasing grade accompanied with enrichment of coexisting amphibole in Fe and Al. Plots of A-site occupancy versus Al^{IV} and Mg versus Al^{IV} (Fig. 6) indicate a gap between actinolite and hornblende. Fig. 6a,b represent hornblende core – actinolite rim, whereas Fig. 6c,d represent actinolite rim – hornblende core. In these diagrams the hornblende is characterized by higher A-site occupancy, higher Al^{IV} and lower Mg.

This gap between the low alumina actinolite and the high alumina hornblende is documented at certain P-T conditions of metamorphism.

However, analyses of unzoned hornblendes from the same sample or other samples (from the same locality) fill this gap (Fig. 4) indicating that the gap actually represents conditions of disequilibrium as discussed in the foregoing paragraphs.

4.2.2. Dependence of amphibole chemistry on bulk rock composition

Using various oxide variation diagrams, a strong positive correlation is observed between the amphiboles and the host rocks for MgO/MgO + FeO and a random distribution for TiO_2, Na_2O and K_2O. For the other oxides the correlation between amphibole and host rock chemistry is not found to be strong, with some positive tendency for CaO, MnO, Al_2O_3, and to some extent SiO_2 (MOGESSIE, 1984).

This implies that for titanium and the alkalies (Na + K) the influence of the pressure and temperature of metamorphism seem to be possibly more significant than the effect of bulk chemistry of the host rock.

4.3. Epidote minerals

Compositions were obtained for epidotes of more than 30 amphibolites. Representative analyses are listed in Table 4. Where zoning has been documented maximum variation in core and rim compositions are also included. The pistacite component (stoichiometric pistacite) $Ca_3(Al,Fe^{3+})Al_2SiO_3O_{12}(OH)$ with the principal variation occurring in $Fe^{3+}/(Fe^{3+}+Al)$ ranges from 5 % to 25,5 % when regionally distributed epidotes are considered together. The increase in Fe^{3+} content (pistacite component) of the epidote-clinozoisite solid solution with decreasing metamorphic grade has been documented by several authors (e. g. MIYASHIRO & SEKI, 1958; ERNST, 1972; HÖRMANN & RAITH, 1973; LIOU et al., 1982).

Since the variation in chemistry of epidotes is mainly dependent on bulk rock chemistry and oxygen fugacity, correlation of changes in epidote composition with changes in metamorphic conditions is difficult. However, examination of the zoned epidotes shades light on the changing metamorphic conditions in the Oetztal-Stubai Basement as has been recorded in other minerals (amphiboles, plagioclase). The only significant chemical variable of the epidote minerals crystallized in the various stages of metamorphism involves substitution of octahedral Al^{VI} and Fe^{3+} as is shown in Fig. 7.

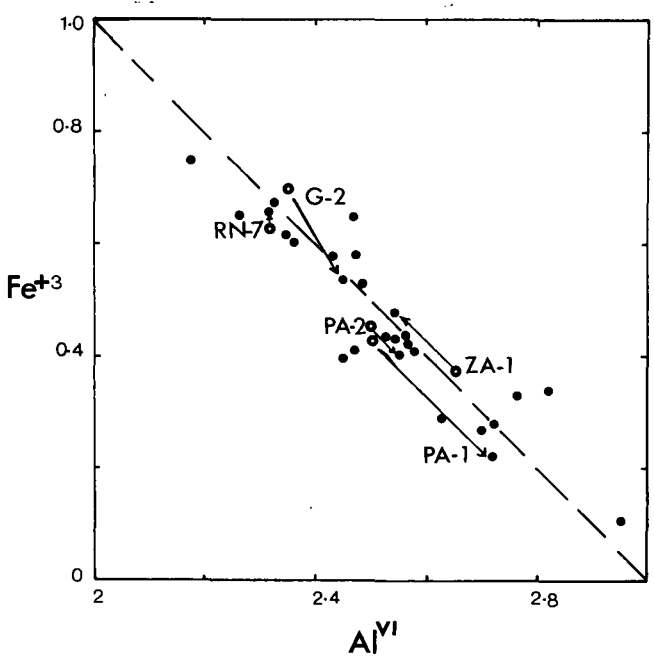

Fig. 7: Proportions of octahedrally coordinated Ferric Iron and Aluminium in epidotes of the Oetztal-Stubai amphibolites. Dashed line indicates ideal substitutions for $Fe^{3+} = Al^{VI}$. Arrows indicate towards rim.

Zoned epidotes from central Oetztal (PA-1, PA-2 from Pollestal) show a lower pistacite content at the rims and a higher amount in the cores suggesting increasing grade of metamorphism. Zoned epidotes from northern Oetztal (ZA-1 from Zirm Alm) show pistacite rich rims and pistacite poor cores indicating a lowering in metamorphic grade.

4.4. Chlorite

Chemical composition of chlorites from several amphibolite samples have been obtained. Representative analyses and structural formulae calculated on the basis of 28 oxygens are listed in Table 5. Plotted on the diagram of HEY (1959) the chlorites are dominantly Pycnochlorite and Ripidolite. The variation of chlorite chemistry seems however to be greatly influenced by extremes in bulk composition (COOPER, 1972). It is also suggested by most authors (e. g. LIOU et al., 1982) that high grade chlorites are consistently more magnesian than greenschist facies chlorites. A comparison of chlorites from central Oetztal and those chlorites from SE Oetztal shows distinct differences in Mg/Fe ratio. Sample MK-3 from Milchenkar with high MgO value in rock (17,9 wt.-%) contains chlorite with Mg/Fe ratio equal to 4,61. Sample WSC-2 from west end of the Schneeberg

Table 4: Representative Electronmicroprobe analyses of epidotes from the amphibolites of the Oetztal-Stubai Basement.

	PA-1		Za-1		G-2	
	core	rim	core	rim	core	rim
SiO_2	38.50	40.46	39.20	39.95	38.95	39.30
TiO_2	0.22	0.00	0.00	0.02	0.10	0.12
Al_2O_3	28.23	29.80	28.89	27.15	24.98	26.37
FeO	7.41	3.73	6.29	8.03	11.60	9.04
MnO	0.17	0.03	0.08	0.00	0.00	0.04
MgO	0.10	0.10	0.06	0.11	0.10	0.17
CaO	25.26	22.92	22.81	21.14	21.48	22.20
K_2O	0.00	0.00	0.00	0.00	0.00	0.00
Na_2O	0.00	0.00	0.00	0.00	0.00	0.00
Total	99.89	97.04	97.33	96.40	97.21	97.24
	Atoms per formula unit based on 12.5 Oxygens					
Si	2.94	3.14	3.06	3.17	3.10	3.10
Al^{IV}	0.06	0.00	0.00	0.00	0.00	0.00
Al^{VI}	2.54	2.72	2.65	2.54	2.35	2.45
Ti	0.01	0.00	0.00	0.00	0.01	0.01
Fe	0.43	0.22	0.37	0.48	0.70	0.54
Mn	0.01	0.00	0.01	0.00	0.00	0.00
Mg	0.01	0.01	0.01	0.01	0.01	0.02
Ca	2.06	1.91	1.90	1.80	1.83	1.87
K	0.00	0.00	0.00	0.00	0.00	0.00
Na	0.00	0.00	0.00	0.00	0.00	0.00
Total	8.06	8.00	8.00	8.00	8.00	7.99
Ps %	14.22	7.37	12.15	15.78	22.73	17.72

Table 5: Representative Electronmicroprobe analyses of chlorites from the amphibolites of the Oetztal-Stubai Basement.

	ZAP-1	PA-1	S-11	KN-4	P21*	P21**
SiO_2	37.83	33.97	35.39	33.38	34.55	35.35
TiO_2	1.49	1.47	2.20	1.65	2.02	2.07
Al_2O_3	16.24	20.21	16.94	19.17	16.75	18.45
FeO	16.05	19.98	20.53	22.88	21.40	16.28
MnO	0.06	0.00	0.06	0.07	0.33	0.12
MgO	13.32	10.25	11.01	8.37	9.87	13.27
CaO	0.08	0.12	0.02	0.80	0.12	0.03
K_2O	8.13	8.33	8.94	7.53	9.08	9.80
Na_2O	0.02	0.00	0.15	0.19	0.12	0.13
Total	93.22	94.33	95.24	94.04	94.24	95.50
	Atoms per formula unit based on 22 Oxygens					
Si	5.7234	5.2108	5.4231	5.2152	5.3936	5.3135
Al^{IV}	2.1054	2.6179	2.3208	2.5889	2.3669	2.4501
Al^{VI}	0.7904	1.0358	0.7387	0.9411	0.7149	0.8184
Ti	0.1713	0.1713	0.2561	0.1958	0.2396	0.2364
Fe	2.0307	2.5630	2.6309	2.9894	2.7937	2.0464
Mn	0.0077	0.0000	0.0078	0.0093	0.0436	0.0153
Mg	3.0032	2.3431	2.5143	1.9488	2.2962	2.9725
Ca	0.0130	0.0197	0.0033	0.1339	0.0201	0.0048
K	1.5691	1.6300	1.7476	1.5008	1.8082	1.8791
Na	0.0059	0.0000	0.0446	0.0576	0.0363	0.0379
Total	15.4201	15.5916	15.6872	15.5808	15.7131	15.7744
Mg/Fe	1.4789	0.9142	0.9557	0.6519	0.8219	1.4525
Mg/Mg+Fe	0.5966	0.4776	0.4887	0.3946	0.4511	0.5923

* Biotite associated with hornblende

** Biotite associated with garnet

Complex with lower MgO value in rock (3 wt.-%) contains chlorite with Mg/Fe ratio equal to 0,9. Texturally, the chlorite in sample WSC-2 is a retrograde product of hornblende showing a deep blue interference colour, whereas the chlorite from Milchenkar is a stable paragenesis which is diminishing in modal amount as a result of the reaction:

actinolite + chlorite + epidote = hornblende

Thus, it can be assumed that both the bulk chemistry of the rock and the P-T conditions of metamorphism have a strong influence on the chemistry of the chlorites.

4.5. Biotite

Representative electronmicroprobe analyses of biotites are presented in Table 6. The biotites as can be seen in the TiO_2 vs. Mg/Fe and Al^{VI} vs. Mg/Fe plots (Fig. 8) are very heterogeneous in aggregate composition, although a small variation occurs in a single specimen. The Mg/Fe ratio ranges from 0,65 to 2,36 and Al^{VI} from 0,65 to 1,15, and MgO from 9,72 to 16,16 wt.-%, FeO from 13 to 19 wt.-%.

The few biotite analyses from the NW and central Oetztal (Hercynian and mixed ages of THÖNI [1981]) plot on the high TiO_2 and low Mg/Fe side. On the Al^{VI} vs. Mg/Fe plot, much cannot be said as the trend for all biotites is, increasing Mg/Fe ratio with almost constant value of Al^{VI}. Such a large chemical variation appears to be due to significant differences in bulk rock composition. According to COOPER (1972) the low Ti, high Al^{VI} and Si are suggested to be characteristic features of greenschist facies biotites from metabasic rock.

The MgO vs. FeO plot (Fig. 8b) shows that the biotites from the SE Oetztal and those biotites from the north (Zirm Alm, sample ZAP-2) believed to be of Alpine age plot on the high MgO side. Biotites from Pollestal (PA-1), Burgstein (S-11) and Kaunertal (KN-4) plot on the high FeO side. Especially significant is the biotite from the Kaunertal sample which plots at the same position as the primary biotites from the Oetztal diabase dikes of RAMMLMAIR (1980).

In sample P-21 where complex zonation of garnets is recorded two different biotite chemistries are also observed (Table 5). The biotites associated with the garnet have high MgO (13,27 wt.-%) and lower FeO (16,28 wt.-%) than the biotites associated with hornblende (MgO = 9,87 wt.-%; FeO = 21,4 wt.-%).

Table 6: Representative Electronmicroprobe analyses of biotites from the amphibolites of the Oetztal-Stubai Basement.

	WSC-2	P-21	S-9	MK-3	KN-5	KN-6
SiO_2	22.66	27.38	26.33	28.46	23.41	28.78
TiO_2	0.04	0.12	0.04	0.00	0.00	0.61
Al_2O_3	25.41	19.94	20.57	18.79	21.46	17.46
FeO	26.12	25.77	16.27	10.78	28.70	19.09
MnO	0.11	0.54	0.14	0.06	0.53	0.35
MgO	13.24	13.08	22.83	27.87	13.42	19.73
CaO	0.11	0.12	0.07	0.05	0.05	1.07
K_2O	0.00	0.00	0.00	0.00	0.00	0.35
Na_2O	0.00	0.64	0.00	0.00	0.03	0.19
Total	87.69	87.59	86.25	86.01	87.60	87.63
	Atoms per formula unit based on 28 Oxygens					
Si	4.8035	5.7848	5.3821	5.6557	5.0698	5.8980
Al^{IV}	3.1901	2.1959	2.6117	2.3443	2.9302	2.0071
Al^{VI}	3.1583	2.7694	2.3440	2.0567	2.5474	2.2101
Ti	0.0064	0.0193	0.0062	0.0000	0.0000	0.0950
Fe	4.6304	4.5532	2.7812	1.7915	5.1978	3.2716
Mn	0.0198	0.0966	0.0242	0.0101	0.0972	0.0608
Mg	4.1825	4.1183	6.9545	8.2537	4.3311	6.0255
Ca	0.0250	0.0272	0.0153	0.0106	0.0116	0.2349
K	0.0000	0.0000	0.0000	0.0000	0.0000	0.0915
Na	0.0000	0.2622	0.0000	0.0000	0.0126	0.0755
Total	20.0159	19.8269	20.1192	20.1226	20.1977	19.9699
Mg/Fe	0.9033	0.9045	2.5005	4.6071	0.8333	1.8418
Mg/Mg+Fe	0.4746	0.4749	0.7143	0.8217	0.4545	0.6481

Two possibilities can be considered to be responsible for these chemical differences:

1) Based on textural grounds the biotites can be considered to be of different generation.
2) Within the rock there could have been sites of mineral growth (Fe-poor) in some parts and (Fe-rich) in others resulting in the different biotite chemistries.

4.6. Garnet

Several hundred analyses of garnets have been made. Representative analyses are presented in Table 7. Generally considered the garnet chemistry ranges, on the basis of endmember formulae; almandine (15–80 %), pyrope (4–32 %), andradite (0–12 %), spessartine (0,12–15 %), and grossular (6–30 %). The garnets from SE Oetztal are characterized by lower pyrope content compared to those of central and NW Oetztal. The maximum pyrope content is obtained from a diablastic garnet amphibolite in Milchenkar, central Oetztal (MK-6 with a pyrope content = 32.29 mol.-%). Representative zoning profiles of these garnets are shown in Figs. 9, 10. The garnets from the Schneeberg Complex (SW–165, Fig. 9a) have zonations that are typically bellshaped, showing progressive depletion of Mn and Ca from core to rim. This exhibits normal zoning of HOLLISTER (1966) and suggests continuous growth of garnet during a single metamorphic episode rather than the more complex zonation patterns of various maxima and minima (e. g. KN-4, and P-21) observed with intermittent growth during multiphase metamorphism (ATHERTON & EDMUNDS, 1966).

This growth of garnet in a single metamorphic episode has also been documented from metapelites of the Schneeberg complex (HOINKES and PURTSCHELLER , 1979; HOINKES, 1978, 1980, TESSARDI, 1981).

Observation of the garnet zoning profiles of samples KN-4 and P-21 (Figs. 9, 10) gives a complex picture of garnet growth in the Oetztal Stubai Basement. Sample KN-4 (from Kaunertal): an inner homogenous core of high CaO, low FeO and MgO with a constant amount of MnO is separated from a rim of low CaO and high FeO, MgO. At the outer rim the MgO still increases and the FeO decreases with a simultaneous increase in CaO.

The sharp break or discontinuity in chemistry especially CaO and FeO from core to rim suggests at least two stages of garnet growth; the core representing an older lower grade metamorphic event and the rim a younger high grade metamorphic event. This garnet profile is also found to be similar to the garnet profiles reported by RÄHEIM (1975) from the Precambrian eclogites in western Tasmania.

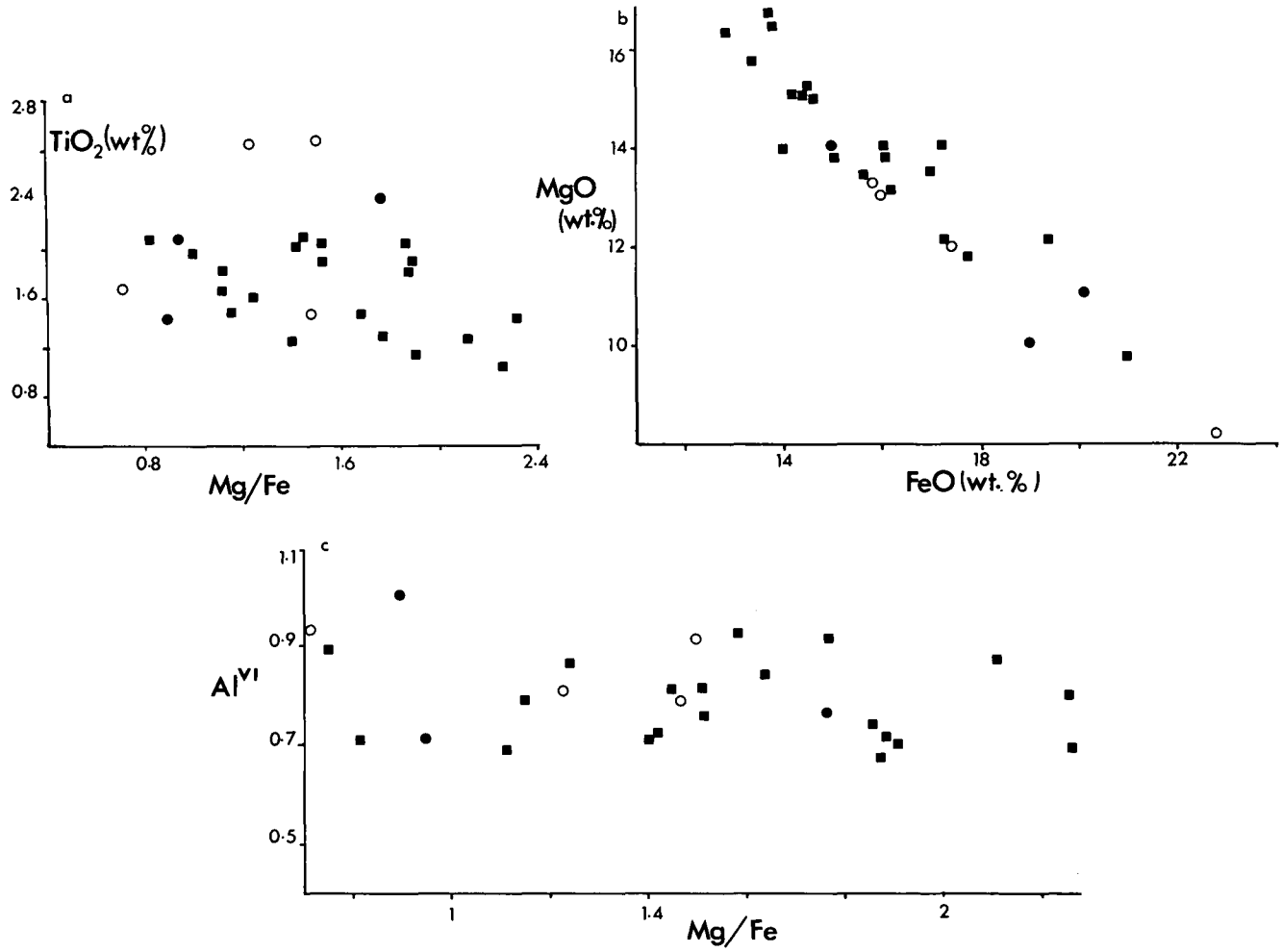

Fig. 8: A plot of (a) TiO_2 vs. Mg/Fe, (b) MgO vs. FeO and (c) Al^{VI} vs. Mg/Fe of biotites from the Oetztal-Stubai amphibolites. Symbols as in Fig. 2.

Sample P-21 (from Pfossental): This sample shows zoning like that of sample KN-4. However, there is a difference in the zoning pattern of the outer rim shown in Fig. 10 (P-21a). The inner cores of the two garnets are characterized by a decrease in CaO and increase in FeO and MgO towards rims. The MnO in this sample shows the same zoning pattern as CaO. At the outer rim the amount of MnO and CaO are found to increase with simultaneous decrease of FeO and a constant MgO value, suggesting a type of resorption or reverse zonation noted by many authors (e. g. GRANT & WEIBLEIN, 1971; DE BETHUNE et al., 1968). Therefore, it may be assumed that this garnet grain from Pfossental represents two main stages of garnet growth like sample KN-4 with a third one resulting from a retrograde process. The two stages of garnet growth have been documented by HOINKES (1980) and TESSARDI (1981) in the rocks of the old crystalline Basement bordering the Schneeberger Zug.

4.6.1. Zoning Pattern of Different Sized Garnet Grains

In a routine electronmicroprobe analyses of garnet grains of different sizes from samples P-21 (Figs. 10a,b&c) a variation in the nature of the zoning pattern is observed. Several other garnet grains from the same sample have been checked in order to evaluate if these different profiles are due to a cut effect of the garnets.

The chemical composition of the garnet interiors vary considerably with size. With diminishing size the inner core of the garnet is disappearing, and the complete profile is displayed by the bigger grains. A similar relation of zoning pattern with garnet size has also been documented by RÄHEIM (1975). ATHERTON & EDMUNDS (1966) have also noted that the most numerous and the smallest crystals are homogeneous while the largest and least numerous show the greatest variation across a crystal. Therefore, if zoning reflects changing conditions of metamorphism, the interpretation of the zoning pattern should take the garnet size into consideration.

5. Interpretation and Discussion

5.1. Polymetamorphism of the Oetztal-Stubai Amphibolites

Based on the rock and mineral analyses, combined with the observed petrographic relationships, the polymetmorphic nature of the Oetztal-Stubai amphibolites is established. Generally, these mineral parageneses can be represented similar to the common mineral assemblages of mafic schist of LAIRD (1980), but in the present case with or without garnet:

Amphibole + chlorite + epidote + plagioclase + quartz + Ti-phase ± carbonate ± garnet ± K-mica ± ± Fe^{3+}oxide

Table 7: Representative Electronmicroprobe analyses of garnets from the amphibolites of the Oetztal-Stubai Basement.

	KN-4		P21		SW-165		Mk-6
	rim	core	rim	core	rim	core	
SiO_2	37.66	37.18	34.46	34.80	38.10	37.61	39.10
TiO_2	0.03	0.15	0.06	0.55	0.00	0.17	0.03
Al_2O_3	23.34	22.60	24.99	24.53	21.60	21.35	22.91
FeO	30.88	29.70	26.59	27.70	30.18	26.18	18.74
MnO	0.36	0.10	3.11	2.60	1.21	3.82	0.53
MgO	5.45	1.83	2.37	2.59	3.58	1.49	8.28
CaO	3.21	8.83	9.06	7.59	5.69	9.91	9.10
K_2O	0.00	0.00	0.00	0.00	0.00	0.00	0.00
Na_2O	0.02	0.03	0.02	0.00	0.02	0.04	0.53
Total	100.95	100.42	100.66	100.36	100.38	100.57	99.22
	Atoms per formula unit based on 24 Oxygens						
Si	5.8563	5.8778	5.4655	5.5253	6.0076	5.9665	5.9592
Al^{IV}	0.1402	0.1042	0.5272	0.4084	0.0000	0.0130	0.0373
Al^{VI}	4.1374	4.1068	4.1441	4.1818	4.0141	3.9789	4.0779
Ti	0.0035	0.0180	0.0072	0.0663	0.0000	0.0205	0.0035
Fe	4.0157	3.9265	3.5268	3.6779	3.9796	3.4732	2.3885
Mn	0.0474	0.0134	0.4178	0.3496	0.1616	0.5133	0.0684
Mg	1.2630	0.4311	0.5602	0.6128	0.8412	0.3523	1.8806
Ca	0.5348	1.4957	1.5396	1.2912	0.9613	1.6845	1.4860
K	0.0000	0.0000	0.0000	0.0000	0.0000	0.0000	0.0000
Na	0.0060	0.0092	0.0062	0.0000	0.0061	0.0123	0.1566
Total	16.0043	15.9827	16.1946	16.1133	15.9715	16.0145	16.0580
Alm	68.52	66.93	58.35	62.01	66.95	57.54	41.01
Andr	0.00	0.00	0.00	0.00	0.00	0.44	0.00
Pyr	21.55	7.35	9.27	10.33	14.15	5.87	32.29
Spess	0.81	0.23	6.91	5.89	2.72	8.55	1.17
Gross	9.13	25.14	25.47	21.77	15.89	27.61	25.52
Uvarov	0.00	0.35	0.00	0.28	0.00	0.00	0.00
Mg/Fe	0.3145	0.1098	0.1588	0.1666	0.2114	0.1014	0.7874
Mg/Mg+Fe	0.2393	0.0989	0.1371	0.1428	0.1745	0.0921	0.4405

LAIRD & ALBEE (1981) suggested that with increasing grade of metamorphism amphibole changes from actinolite-hornblende-tschermakite; meaning Na^A, K, Na^{M4}, Al^{VI}, Ti, (Al^{VI} + Fe^{3+} + Ti + Cr) and Al^{IV} contents increase. Plagioclase becomes more anorthitic with metamorphic grade.

The zoned calcic amphiboles of the Oetztal-Stubai amphibolites represent various combinations of core-rim composition, i. e. actinolite-hornblende; hornblende-actinolite. These types of textural relationships are considered to indicate multiple periods of mineral growth (LAIRD & ALBEE, 1981). The cores appear to be relics, preserved because of incomplete equilibration.

Textural relations show that the calcic amphiboles of the Oetztal-Stubai amphibolites represent at least four different periods of mineral growth as given below:

1) High-alumina calcic amphiboles (stage I) within diablastic garnet amphibolites (retrograde products of eclogites).
2) Low-alumina actinolite core (stage II) rimmed by Al-rich calcic amphibole (stage III).
3) Al-rich calcic amphibole (stage III) rimmed by low-alumina actinolite (stage IV).

The other minerals, garnet and plagioclase also show the same zoning pattern like the amphiboles indicating changing metamorphic conditions.

In order to evaluate the different growth periods of the zoned minerals of the Oetztal-Stubai amphibolites and conclude a sequence of metamorphic events, some suggested models for the evolution of the Eastern Alps, especially the Oetztal-Stubai Basement are considered.

PURTSCHELLER & SASSI (1975) suggested the following succession of events in the Oetztal-Stubai Complex:

1) Basic magmatism
2) High pressure metamorphism
3) Granitoid plutonism, of certainly Caledonian age (415–486 m.y.)
4) Retrograde phase
5) Tectonic activity
6) Metamorphism of rather low pressure, of Hercynian age (Rb-Sr-cooling ages around 300 m. y.) and related post kinematic Hercynian anatexis.

They considered events 1,2,3 and possibly 4 to make up the Caledonian cycle. Event 6 would represent the Hercynian cycle. The chronological attribution of event 5 is uncertain. They also suggested that the regional Caledonian metamorphism to have ended with a low temperature high P_{H_2O}phase, whose age could be early Hercynian.

The compositionally and texturally distinct calcic amphiboles outlined above could fit the evolutionary model. The high alumina calcic amphiboles, because of

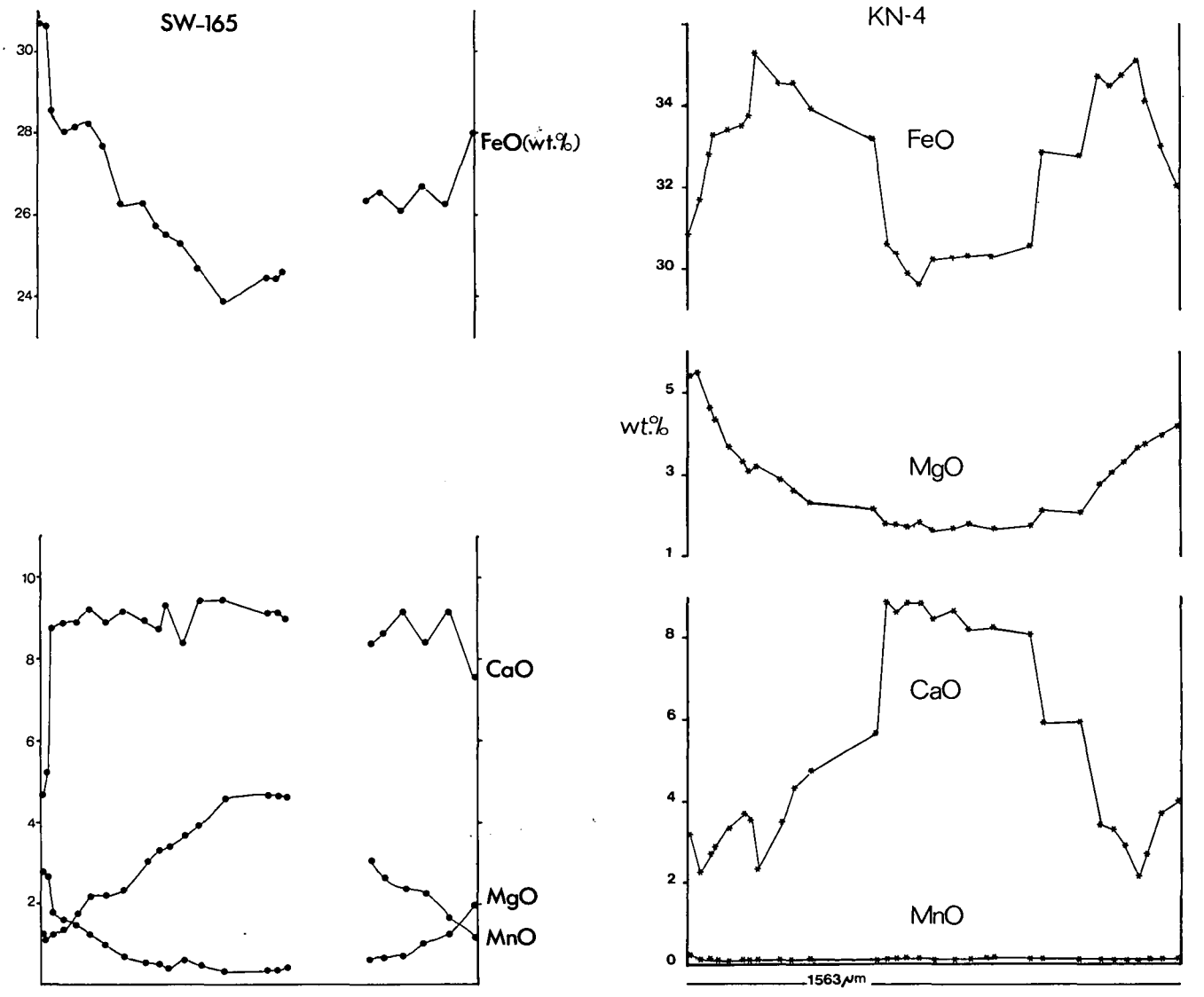

Fig. 9: a) Zoning profile of garnet from the Schneeberger Zug amphibolites; sample SW-165, showing a bell-shaped zoning pattern of progressive metamorphism; b) Zoning profile of garnet; sample KN-4 from Kaunertal, representing two generations of garnet growth.

their occurrence within diablastic garnet amphibolites are considered to be the oldest calcic amphiboles of the Oetztal-Stubai amphibolites. Thus, they could be assigned to an older pre-Hercynian age which could possibly be Caledonian.

The occurrence of a low grade (greenschist facies) mineral parageneses which could be late Caledonian or early Hercinian age has not been documented heretofore in this part of the eastern Alps. However, the polyphase nature of the Hercynian event has been considered by many authors (FRANK et. al., 1978).

As can be seen from the evolutionary model (PURTSCHELLER & SASSI, 1975) the age of event 4 was questionable but it has been suggested that the end of the Caledonian event is characterized by a low temperature and high P_{H_2O}. Thus, the actinolite core may be considered to have grown at this stage which may reflect a P-T condition of the greenschist facies.

In central Oetztal actinolite rim-hornblende core relations are observed in samples PA-4 from Pollestal, MK-8 from Milchenkar. Based on the decreasing nature of the Alpine metamorphism towards the NW, (PURTSCHELLER & RAMMLMAIR, 1981), the actinolite rims represent the effect of the Alpine overprint on the original Hercynian amphibolite facies parageneses. The same is true for the actinolite rim hornblende core relations observed in samples DO-417, DO-420, ZAP-1, ZAP-2 from Sellraintal; LS-1, LS-5 from Lüsens.

However, the hornblende core in samples RL (Rotmoostal), L-37 (Gaisbergtal), LT-126 (Langtal) represent the Alpine amphibolite facies overprint on the Hercynian parageneses, which in principle has equilibrated at similar P-T conditions of metamorphism, (Alpine temperatures of 550°C are suggested, RAMMLMAIR (1980), PURTSCHELLER & RAMLMAIR (1981), HOINKES (1980). The actinolite rim in these samples is assumed to be the result of the early Alpine cooling, in agreement with the garnet zoning in Pfossental (Fig. 10, sample P-21).

In order to have a clear picture of the nature of the polymetamorphism of the Oetztal-Stubai amphibolites the actinolite core-hornblende rim and the actinolite rim hornblende core relations are presented in Fig. 11 of LAIRD & ALBEE (1981). In this diagram the Na-side indicates increasing pressure and the Al-side increasing temperature of metamorphism. The actinolites plot on the low Na × 100/Na + Ca and Al × 100/Al + Si side and the Al-rich amphiboles on the high Al and Na-side.

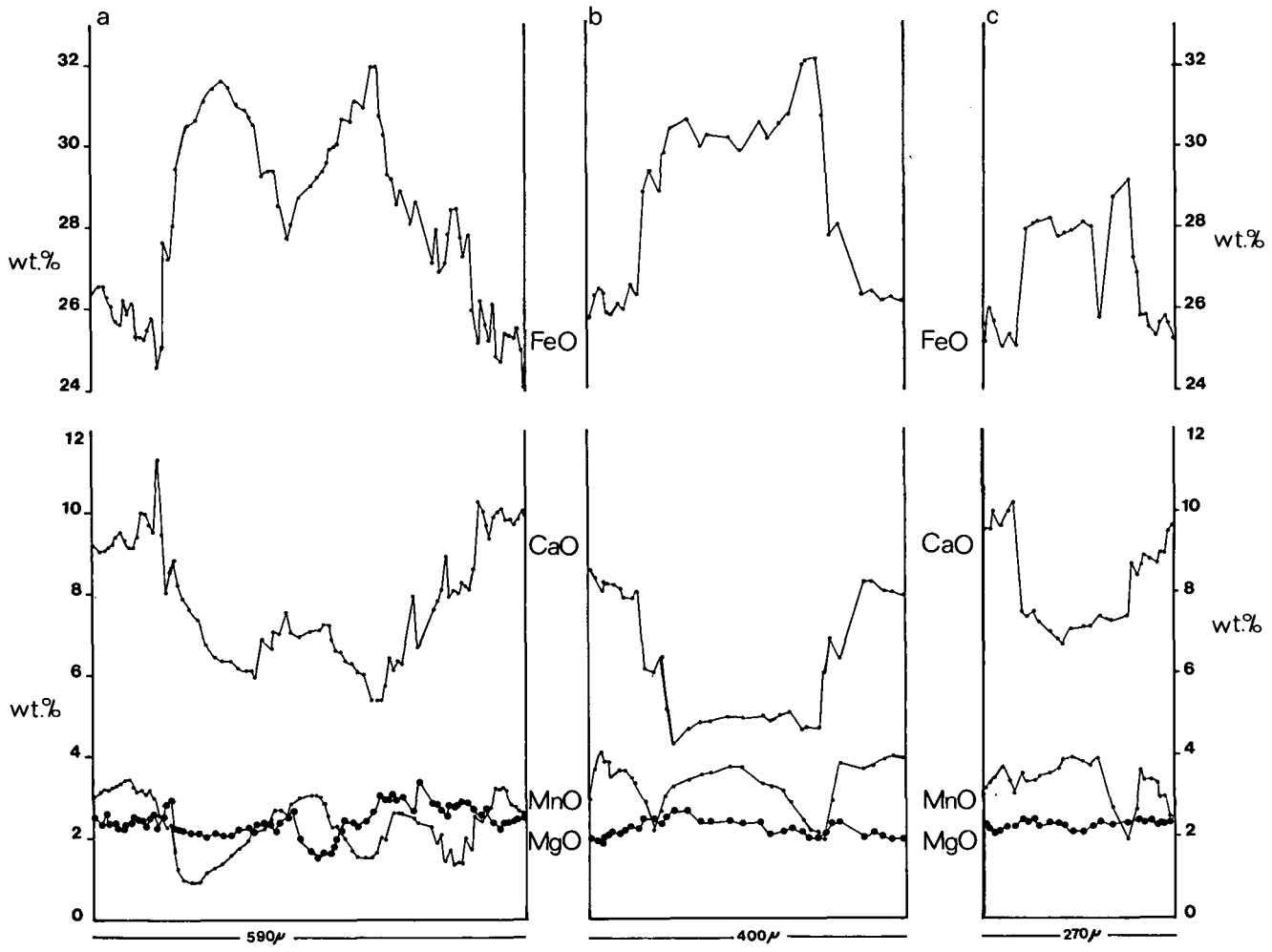

Fig. 10: Zoning profiles (a,b,c) of different sized garnets from sample P-21 (Pfossental). The zoning depends on the size of the garnet. The bigger the garnet (a) the three different stages of garnet growth are recorded. The inner core diminishes with decreasing size of the garnet as in (b) and (c).

The arrows indicate the path of metamorphic processes that have been effective in the Oetztal-Stubai Complex as discussed above. The petrolocic description and age assignments of the mineral growth events are tabulated below (Table 8).

5.2. Physical Conditions of Metamorphism

The various mineral growth periods and the mineral parageneses representing these periods are considered below in terms of the physical conditions of metamorphism and comparison with other experimental and petrographic studies.

Phase relations between greenschist and amphibolite facies mineral assemblage for basaltic bulk-composition have been investigated both in the field and in the laboratory (COOPER, 1972; LIOU et al., 1974; KUNIYOSHI & LIOU, 1976; SPEAR, 1980, 1981; LIOU et al., 1982). The stability of hornblende and the associated phases for an olivine tholeiite composition has been determined by SPEAR (1981). These experimentally determined stabilities as well as the characteristic mineral assemblage for the olivine tholeiite composition are presented in Fig. 12. On this P-T diagram the positions of the amphibolite assemblages and their retrograde products (greenschist equivalents) are indicated and the P-T conditions of formation estimated.

The amphibolites are characterized by hornblende + plagioclase + epidote + sphene ± ilmenite ± garnet ± quartz. Sphene occurs in most of the amphibolites suggesting that the amphibolite assemblage is bounded by the sphene-out reaction at high temperature and the chlorite-out reaction at low temperature. Thus, the amphibolite metamorphism took place between 550°C and 700°C and at values of P_f on the order of 5Kb. These values are in agreement with the P-T data of HOINKES et al. (1972) for the Hercynian metamorphism in this part of the Oetztal Alps. (T = 670°C, P = 3–4Kb).

The amphibolites are recrystallized to actinolite + albite + epidote + quartz + chlorite ± biotite + sphene as a result of the Alpine overprint. Because of the occurrence of both the amphibolite assemblages and their retrograde greenschist assemblages in all the studied samples, and the fact that a calcic plagioclase (An_{40}) is found altering to pure albite (An_1), the temperature of metamorphism for the Alpine overprint in central Oetztal is assumed to be within the range 475°C–550°C, representing the transition zone between the greenschist and the amphibolite facies.

Occurence of biotite as a retrograde product in these samples also suggest a metamorphic condition characteristic of the upper greenschist facies. IN SE Oetztal the Alpine overprint is characterized by amphibolite facies assemblages hornblende + plagioclase; and a

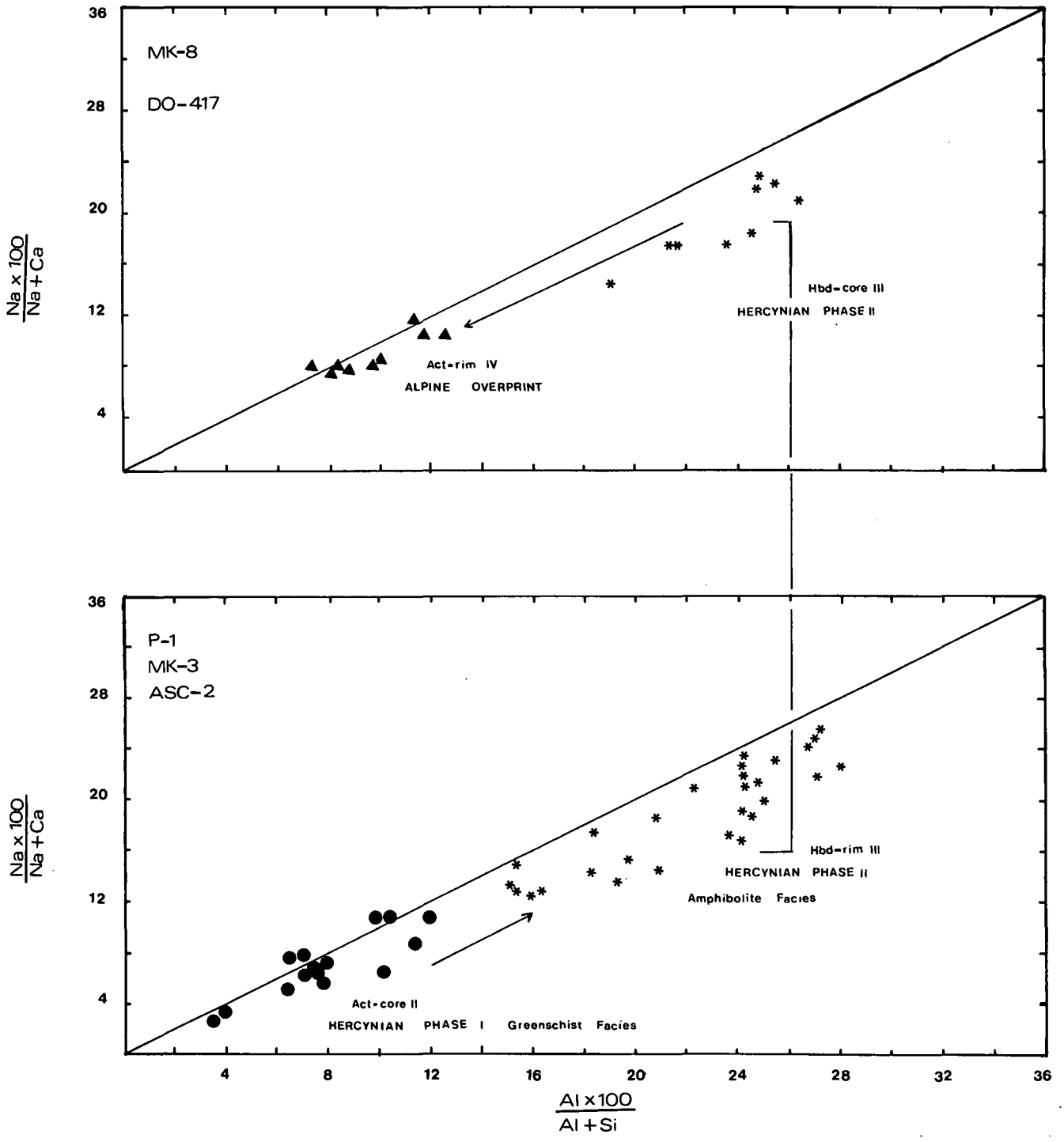

Fig. 11: Actinolite core (Hercynian phase I), hornblende rim (Hercynian phase II) and actinolite rim (Alpine overprint) relations indicating the nature of the polymetamorphism of the Oetztal-Stubai amphibolites.

temperature greater than 550°C is suggested, in agreement with PURTSCHELLER & RAMMLMAIR (1981) and HOINKES (1980).

6. Conclusion

Based on the rock and mineral analyses and the observed petrographic relationships, evidence for the polymetamorphic nature of the Oetztal-Stubai amphibolites have been established. In central Oetztal and NW, low-K tholeiitic gabbros, in SE possible tuffaceous material (MOGESSIE et al., 1985) have been subjected to different grades of metamorphism at different stages to produce the presently exposed amphibolitic units. In the NW and central Oetztal amphibolites with or without garnet associated with eclogites, peridotites and metagabbros occur. These associated gabbros of tholeiitic composition and the ultramafics could be ocean floor rocks. The nature of the transformation from eclogite to amphibolite can be observed in a series of hand specimen and with the miscroscope, from a garnet + pyroxene to a hornblende + plagioclase assemblage. The occurrence of relict high alumina clacic amphiboles enclosed within garnets of eclogite and diablastic gar-

Table 8: Petrologic description and age assignments of mineral growth events in amphibolites of the Oetztal-Stubai complex.

Event	Isotopic age	Grade	Locations	Sample	Amphiboles	Other diagnostic minerals	Facies Series
Caledonian	430–500 my.	Eclogite, Kyanite	Central Oetztal	PA-3, S-5, PA-2, MK-6	High Al-Hbd. (I)	Garnet, Zoisite, Kyanite, Omphacite	High Pressure
Hercynian	300–360 my.	Sillimanite, Kyanite	Central Oetztal	MK-3, PA-42	Act-core (II) Hbd-rim (III)		Medium Pressure
		Andalusite, Sillimanite	NW-Oetztal	KN-1, PZ-3	Act-core (II) Hbd-rim (III)		Low Pressure
		Kyanite	SE-Oetztal	ASC-2	Act-core (II) Hbd-rim (III)		Medium Pressure
Alpine overprint	100–80 my.	Sillimanite, Kyanite	Central Oetztal	PA-4, MK-8	Hbd-core (III) Act-rim (IV)	Albite	Medium Pressure
		Kyanite	N-Oetztal	ZAP-1, ZAP-2 Do 417, Do 420	Hbd-core (III) Act-rim (IV) Hbd-core (III) Act-rim (IV)	Albite Albite rimming Calcic feldspar	
		Kyanite	NE-Oetztal	RN-7, FI-2	Hbd-core (III) Act-rim (IV)	Albite	
Alpine	100–80 my	Kyanite Staurolite, Kyanite	SE-Oetztal Schneeberger Zug	L-37, Lt-126 SW-185 PL-83	Hbd-core $(III)_a$ Act-rim*) Hbd Hbd	Albite Oligocl. – And. Oligocl. – And.	Medium Pressure

*) Early Alpine cooling.
Those underlined refer to the Hercynian metamorphic events.
Hbd-core $(III)_a$ refers to the Alpine overprint in SE = the Hercynian (in this region).

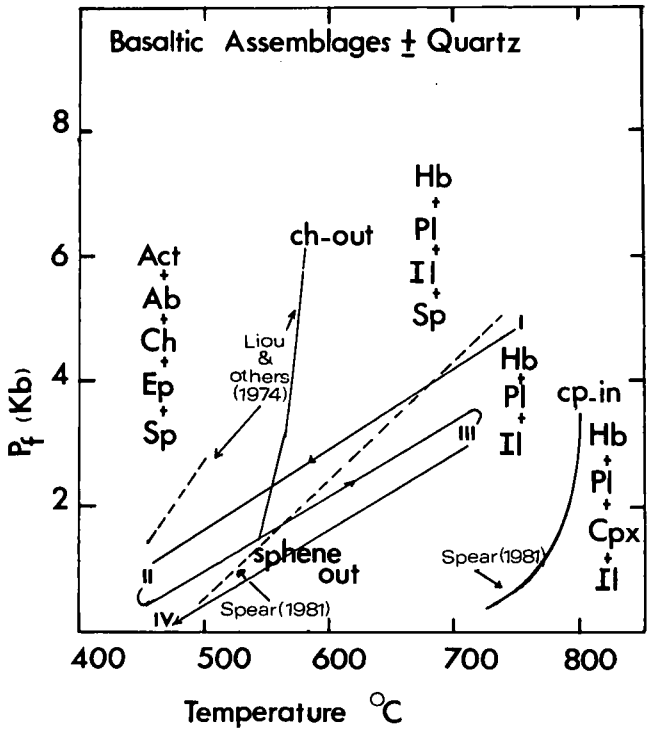

Fig. 12: P_{fluid}-T diagram showing stability relations of mineral assemblages for various metamorphic facies in system of basaltic composition. Experimentally determined stabilities are shown for Chlorite-decreasing and Chlorite-out (LIOU et al., 1974), Sphene-out and Clinopyroxene-in for basaltic compositions (SPEAR, 1981). Basaltic assemblages ± quartz for various P_f-T conditions are also shown.
Act = actinolite, Chl = chlorite, Sp = sphene, Pl = plagioclase, Hb = hornblende, Il = ilmenite, Cpx = clinopyroxene.
The estimated P-T regions for the different texturally and chemically distinct calcic amphiboles of the Oetztal-Stubai amphibolites are also indicated.
I = high alumina calcic amphibole (pre-Hercynian); II = actinolite core (Hercynian phase I); III = alumina rich calcic amphibole (Hercynian phase II; IV = actinolite rim (Alpine overprint). The Alpine overprint in SE Oetztal is comparable to Hercynian phase II.

net amphibolites suggest that some of these amphibolites record mineral parageneses of pre-Hercynian or possible Caledonian age.

The change from actinolite + chlorite + epidote + quartz (a greenschist facies assemblage) to a hornblende + plagioclase (amphibolite facies) during the Hercynian stage of metamorphism, followed by a complex relation of possible Hercynian retrograde parageneses/Alpine overprint are documented. The Hercynian greenschist facies (phase I or stage II) and the Hercynian amphibolite facies (phase II or stage III) mineral assemblages may be related to the regional metamorphism and associated tectonic breaks during the Carboniferous and the permian respectively (MOSTLER personal communication).

The polymetamorphic situation in the Oetztal-Stubai amphibolites can be summarized as follows:

1) A high P & T metamorphism of pre-Hercynian age.
2) A low grade greenschist facies metamorphism of possible early Hercynian age (phase I)-Carboniferous.
3) A low to medium P and high T amphibolite facies metamorphism of Hercynian age (phase II)-Permian; with a maximum in central Oetztal and decreasing towards the N and the SE, but still remaining within the amphibolite facies.
4) An Alpine overprint whose metamorphic grade decreases from SE Oetztal towards the NW, of Cretaceous age.
5) Early Alpine cooling (represented by retrograde mineral assemblages in amphibolites of the old crystalline Basement bordering the Schneeberger Zug).

Acknowledgements

We would like to express our thanks to Univ. Prof. Dr. H. MOSTLER (Institute of Geology and Palaeontology, University of Innsbruck), Univ. Doz. Dr. G. HOINKES and Dr. R. TESSADRI (Institute of Mineralogy and Petrography, University of Innsbruck) for critically reviewing the Manuscript. This work was supported by the Fonds zur Förderung der Wissenschaftlichen Forschung in Österreich (project S 15 & P 4843).

Appendix

Location of samples studied (Oetztal-Stubai Basement).

Sample	Locality	Rock Type
PZ-1	Pitztal	Garnet Amphibolite
PZ-2	Pitztal	Garnet Amphibolite
PZ-3	Pitztal	Epidote Amphibolite
PZ-4	Pitztal	Amphibolite
PZ-5	Pitztal	Amphibolite
KN-1	Kaunertal	Amphibolite
KN-4	Kaunertal/Ober Kaltenbrunn	Eclogite-Amphibolite
KN-5	Kaunertal/Ober Kaltenbrunn	Garnet Amphibolite
KN-6	Kaunertal/Ober Kaltenbrunn	Garnet Amphibolite
St-3	Kaunertal near the dam	Amphibolite
P-1	Prämayur	Amphibolite
N 494	near Kühtai	Amphibolite
ZAP-1	near Zirm Alm	Amphibolite
ZAP-2	near Zirm Alm	Amphibolite
ZA-1	near Zirm Alm	Amphibolite
ZA-9	near Zirm Alm	Garnet Amphibolite
Do-417	Sellraintal/Silz	Amphibolite
Do-420	Sellraintal/Silz	Amphibolite
RN-3	Ranalt	Garnet Amphibolite
RN-4	Ranalt	Amphibolite
RN-7	Ranalt	Epidote Amphibolite
LS-1	Lüsens	Garnet Amphibolite
LS-4	Lüsens	Amphibolite
LS-4	Lüsens	Amphibolite
PA-1	Pollestal Alm	Diablastic Garnet Amphibolite
PA-2	Pollestal Alm	Diablastic Garnet Amphibolite
PA-3	Pollestal Alm	Eclogite Amphibolite
PA-4	Pollestal Alm	Amphibolite
PA-42	Pollestal Alm	Amphibolite
MK-1	Milchenkar	Amphibolite
MK-3	Milchenkar	Amphibolite
MK-6	Milchenkar	Diablastic Garnet Amphibolite
MK-8	Milchenkar	Amphibolite
S-2	Sölden	Eclogite Amphibolite
S-3	Sölden (before the tunnel in the direction of Längenfeld)	Eclogite Amphibolite
S-4	Sölden (before the tunnel in the direction of Längenfeld)	Eclogite Amphibolite
S	Aschbach near Sölden	Amphibolite
S-5	Sölden	Garnet Amphibolite
S-6	Sölden	Epidote Amphibolite
S-7	Sölden	Epidote Amphibolite
S-8	Burgstein near Längenfeld	Garnet Amphibolite
S-9	Burgstein near Längenfeld	Amphibolite
S-10	Burgstein near Längenfeld	Garnet Amphibolite
S-11	Burgstein near Längenfeld	Garnet Amphibolite
VN-1	Ventertal	Amphibolite
R 6	Rotmoostal	Garnet Amphibolite
RL	Rotmoostal	Amphibolite
ASC-1	Pfossental near Eishof	Garnet Amphibolite
ASC-2	Pfossental near Eishof	Amphibolite

Wsc-1	Pfossental (western end of Schneeberger Zug)	Amphibolite
Wsc-2	Pfossental (western end of Schneeberger Zug)	Garnet Amphibolite
P-17	Pfossental	Garnet Amphibolite
P-21	Pfossental	Garnet Amphibolite
P-26	Pfossental	Garnet Amphibolite
FL-1	Fotschertal	Amphibolite
FL-2	Fotschertal	Amphibolite
G-1	Gaisbergtal	Garnet Amphibolite
G-2	Gaisbergtal	Epidote Amphibolite
O-21	Gaisbergtal	Garnet Amphibolite
L-37	Gaisbergtal	Amphibolite
LT-126	Langtal	Amphibolite
F-89	Festkogel	Garnet Amphibolite
F-5	Festkogel	Garnet Amphibolite
F-44	Festkogel	Garnet Amphibolite
F-78	Festkogel	Amphibolite
SW-165	Seebertal	Garnet Amphibolite
SW-170	Seebertal	Garnet Amphibolite
SW-185	Seebertal	Garnet Amphibolite
PL-83	Pfelderertal	Garnet Amphibolite
PL-95	Pfelderertal	Garnet Amphibolite
J-6	Jaufen Pass	Amphibolite

References

ATHERTON, M. P. & EDMUNDS, W. M.: An Electronmicroprobe study of some zoned garnets from metamorphic rocks. – Earth Planet Sc. Letters, 185–193, Amsterdam 1966.

BENCE, A. E. & ALBEE, A. L.: Emperical correction factors for the electron probe micro-analyses of silicates and oxides. – J. Geol., **76**, 382–403, Chicago 1968.

BETHUNE de, P., LADURON, D., MARTIN, H. & THEUNISSEN, K.: Grenates zonés de la zone du Mont Rose (Valla Anzasca, prov de Novara Italie). – SMPM., **48**, 437–454, Zürich 1968.

BRADY, J. B.: Coexisting actinolite and hornblende from west central New Hampshire. – Am. Mineralogist., **59**, 529–535, Richmond Virginia 1974.

COMPTON, P. R.: Significance of amphibole parageneses in the Bidwell Bar region, California. – Am. Mineralogist, **43**, 890–907, Richmond Virginia 1958.

COOPER, A. F. & LOVERING, J. F.: Greenschist amphiboles from Haast River New Zealand. – Contrib. Mineral. Petrol., **27**, 11–24, Berlin 1970.

COOPER, A. F.: Progressive metamorphism of metabasite rocks from the Haast schist group of southern New Zealand. – J. Petrol., **13**, 457–492, Oxford 1972.

DOOLAN, B. L., DRAKE, J. C. & CROCKER, D.: Actinolite and subcalcic hornblende from a greenstone of the Haazanś Notsch Formation Lincoln Mtn. Quadr., Warren, Vermont (Abs.). – Geol. Soc. Am. N. E. Sect. 8th Ann. Meet., Abs. progr., **2**, 157, 1973.

ERNST, W. G.: Ca-amphibole paragenesis in the Shirataki district central Shikoku, Japan. – In: Studies in mineralogy and precambrian geology: The John W. Gruner Volume, (eds. DOE, B. R. & SMITH, D. K.) Geol. Soc. Am. Mem., **135**, 73–194, 1972.

FRANK, W., PURTSCHELLER, F., SASSI, F. P. & ZANETTIN, B.: Eastern Alps. – In: Metamorphic Map of the Alps 1 : 1.000.000, Explanatory text (Compiled by E. NIGGLI), 228–237, Leiden 1978.

GRAHAM, C.: Metabasite amphiboles of the Scottish Dalradian. – Contrib. Mineral. Petrol., **47**, 165–185, Berlin 1974.

GRANT, J. A. & WEIBLEIN, P. W.: Retrograde zoning in garnet near the second Sillimanite isograde. – Am. J. Sci., **270**, 281–296, New Haven, Connecticut 1971.

GRAPES, R. H.: Actinolite-hornblende pairs in metamorphic gabbros, Hidaka Mountains, Hokkaido. – Contrib. Mineral. Petrol., **49**, 125–140, Berlin 1975.

GRAPES, R. H. & GRAHAM, C. M.: The actinolite-hornblende series metabasites and the so-called miscibility gap: a review. – Lithos., **11**, 85–97, Oslo 1978.

HALLIMOND, A. F.: On the graphical representation of the calciferous amphiboles. – Am. Mineralogist., **28**, 65–89, Richmond, Virginia 1943.

HIETANEN, A.: Amphiboles pairs, epidote minerals, chlorite and plagioclase in metamorphic rocks, northern Sierra Nevada, California. – Am. Mineralogist., **59**, 22–40, Richmond, Virginia 1974.

HEY, M. H.: A new review of chlorites. – Min. Magazine., **30**, 277–292, London 1954.

HEZNER, L.: Beitrag zur Kenntnis der Amphibolite und Eklogite. – TMPM., **22**, 437–471, 505–580, Vienna 1903.

HIMMELBERG, G. R. & PAPIKE, J. J.: Coexisting amphiboles from blueschist facies metamorphic rocks. – J. petrol., **10**, 102–114, Oxford 1969.

HOERNES, S. & HOFFER, E.: Der Amphibolitzug des mittleren Ötztales (Tirol). – Veröff. Museum Ferdinandeum Ibk., **53**, 159–180, Innsbruck 1973.

HOFFER, E.: Der Amphibolitzug des Geigenkammes im mittleren Ötztals. – Diss. Innsbruck 1967.

HOINKES, G., PURTSCHELLER, F. & SHANTL, J.: Zur Petrographie und Genese des Winnebachgranites (Ötztaler Alpen, Tirol). – TMPM., **18**, 292–311, Vienna 1972.

HOINKES, G.: Zur Mineralchemie und Metamorphose toniger und mergeliger Zwischenlagen in Marmoren des südwestlichen Schneebergerzuges (Ötztaler Alpen, Südtirol). – N. Jb. Miner. Abh., **131**, 272–303, Stuttgart 1978.

HOINKES, G. & PURTSCHELLER, F.: Zur Metamorphose des Schneebergerzuges. – Tiefbau der Ostalpen, Jahresbericht, **7**, 11–16, Zentralanstalt Meteorol. Geodyn., Vienna 1977.

HOINKES, G.: Mineralogie und Metamorphose im westlichen Schneebergerzug und angrenzenden Altkristallin. – Habilitationsschrift, Innsbruck 1980.

HOINKES, G.: Mineralreaktionen und Metamorphosenbedingungen in Metapeliten des westlichen Schneeberger Zuges und des angrenzenden Altkristallins (Ötztaler Alpen). – TMPM, **28**, 31–54, Vienna 1981.

HOINKES, G., PURTSCHELLER, F. & TESSADRI, R.: Polymetamorphose im Ostalpin westlich der Tauern (Ötztaler Masse, Schneeberger Zug, Brennermesozoikum). – Geol. Paläont. Mitt. Innsbruck, **12**, 95–113, Innsbruck 1982.

HOINKES, G.: Cretaceous metamorphism of metacarbonates in the Austroalpine Schneeberger Complex, Tyrol. – SMPM, **63**, 95–114, Zürich 1983.

HOLLISTER, L. S.: Garnet Zoning: An interpretation, based on the Rayleigh Fractionating model. – Science, **154**, 1647–1651, Washington D. C. 1966.

KLEIN, C. Jr.: Two amphibole assemblages in the system actinolites – hornblende – glaucophane. – Am. Mineralogist., **54**, 212–237, Richmond, Virginia 1969.

KUNIYOSHI, S. & LIOU, J. G.: Contact metamorphism of the Karmutsen volcanics, Vancouver Island, British Columbia. – J. Petrol., **17**, 73–99, Oxford 1976.

LAIRD, J.: Phase equilibratia in mafic schist from Vermont. – J. Petrol., **21**, 1–37, Oxford 1980.

LAIRD, J. & ALBEE, A. L.: Pressure, temperature and time indicators in mafic schist: their application to reconstructing the polymetamorphic history of Vermont. – Am. J. Sci., **281**, 127–175, New Haven, Connecticut 1981.

LEAKE, B. E.: The relationship between tetrahedral aluminium and the minimum possible octahedral aluminium in natural calciferous and subcacliferous amphiboles. – Am. Mineralogist., **50**, 843–851, Richmond, Virginia 1965.

LEAKE, B. E.: Nomenclature of amphiboles. – Am. Mineralogist., **63**, 1023–1052, Richmond, Virginia 1978.

LIOU, J. G., KUNIYOSHI, S. & ITO, K.: Experimental studies of the phase relations between greenschist and amphibolite in a basaltic system. – Am. J. Sci., **274**, 613–632, New Haven, Connecticut 1974.

LIOU, J. G., ERNST, W. G. & MOORE, D. E.: Geology and petrology of some polymetamorphosed amphibolites and associated rocks in north-eastern Taiwan. – Geol. Soc. Am. Bull., Part II, 609–748, Colorado 1982.

MILLER, C. H.: Petrology of some eclogites and metagabbros of the Oetztal Alps, Tyrol, Austria. – Contrib. Mineral. Petrol., **28**, 42–56, Berlin 1970.

MIYASHIRO, A. & SEKI, Y.: Enlargement of the composition field of epidote and piemontite with rising temperature. – Am. J. Sci., **256**, 423–430, New Haven, Connecticut 1958.

MOGESSIE, A.: Petrology and Geochemistry of the Oetztal-Stubai Amphibolites, Eastern Alps (Tyrol, Austria). – Ph. D. Thesis, University of Innsbruck (unpublished), Innsbruck 1984.

MOGESSIE, A. & TESSADRI, R.: A basic computer program to determine the name of an amphibole from an electronmicroprobe analyses. – Geol. Paläont. Mitt. Innsbruck, **11**, 259–289, Innsbruck 1982.

MOGESSIE, A., PURTSCHELLER, F. & TESSADRI, R.: Geochemistry of amphibolites from the Oetztal-Stubai Complex (Northern Tyrol, Austria). – Chem. Geol., **51**, 103, Amsterdam 1985.

PURTSCHELLER, F.: Mineralzonen im Ötztaler-Stubaier Altkristallin. – Österr. Akad. Wiss., math.-naturw. Kl., **2**, Vienna 1967.

PURTSCHELLER, F.: Petrographische Untersuchungen an Alumosilikatgneisen des Ötztaler-Stubaier Altkristallins. – TMPM, **13**, 35–54, Vienna 1969.

PURTSCHELLER, F. & SASSI, F. P.: Some thoughts on the pre-alpine metamorphic history of the austridic Basement of the Eastern Alps. – T. M. P. M., **22**, 175–199, Vienna 1975.

PURTSCHELLER, F.: Ötztaler und Stubaier Alpen. Sammlg. – 2. Aufl., Geol. Führer, **53**, Berlin – Stuttgart (Borntraeger) 1978.

PURTSCHELLER, F. & RAMMLMAIR, D.: Alpine metamorphism of diabase dikes in the Oetztal-Stubai metamorphic complex. – T. M. P. M., **29**, 205–221, Vienna 1981.

PURTSCHELLER, F., HOINKES, G., RAMMLMAIR, D., TESSADRI, R. & DIETRICH, H.: Bericht über petrologische Neuergebnisse im Brennermesozoikum, Schneeberger Zug und Altkristallin im Jahre 1979. – Jahresber. **1979**, Hochschulschwerpunkt S 15, H. **1**, 84–85, Leoben 1979.

RÄHEIM, A.: Mineral zoning as a record of P-T history of precambrian eclogites and schists in western Tasmania. – Lithos., **8**, 221–236, Oslo 1975.

RAMMLMAIR, D.: Petrographie der Diabase der Ötztaler/Stubaier Masse. – Diss. Univ. Innsbruck, Innsbruck 1980.

SHIDO, F.: Plutonic and metamorphic rocks of the Nokoso Iritono districts in the central Abukuma Plateau. – J. Fac. Sci. Univ. Tokyo, Sect. II, **11**, 131–217, Tokyo 1958.

SMULUKOWSKI, W.: Amphiboles and biotite in relation to the stages of metamorphism in granogabbro. – Min. Magazine, **39**, 857–866, London 1974.

SÖLLNER, F. & SCHMIDT, K.: Rb/Sr- und U/Pb-Datierungen am Winnebach Migmatit (Ötztaler Alpen, Österreich). – Fortschr. Mineral., **59**, Beiheft 1, Stuttgart 1981.

SPEAR, F. S.: NaSi = CaAl exchange equilibrium between plagioclase and amphibole. – Contrib. Mineral. Petrol., **72**, 33–41, Berlin 1980.

SPEAR, F. S.: an experimental study of hornblende stability and compositional variability in amphibolite. – Am. J. Sci., **281**, 697–734, New Haven, Connecticut 1981.

STOUT, J. H.: Phase petrology and mineral chemistry of coexisting amphiboles from Telemark, Norway. – J. Petrol., **13**, 99–145, Oxford 1972.

TESSADRI, R.: Zur Metamorphose am Ostende des Schneeberger Zuges (Sterzing/Südtirol). – Unpubl. Diss. Univ. Innsbruck, Innsbruck 1981.

THÖNI, M.: Distribution of pre-Alpine and Alpine metamorphism of the southeastern Oetztal mass and the Scarl Unit, based on K/Ar age determinations. – Mitt. Geol. Ges. Wien, **71/72**, 139–165, Vienna 1980.

THÖNI, M.: Degree and evolution of the Alpine metamorphism in the Austroalpine Unit west of the Hohe Tauern in the light of K/Ar and Rb/Sr age determinations on micas. – Jb. Geol. B.-A., **124**, 111–174, Vienna 1981.

Manuskript bei der Schriftleitung eingelangt am 17. Juni 1985.